AMERICAN UNIVERSITY OF BEIRUT

COMPARATIVE EFFECTS OF PARTHENOLIDE AND A SESQUITERPENE LACTONE FROM *COTA PALAESTINA SUBSP. SYRIACA* ON TUMOR PHENOTYPE OF MDA-MB-231 BREAST ADENOCARCINOMA CELLS

by
BILAL NASSIB NASR

A thesis
submitted in partial fulfillment of the requirements
for the degree of Master of Science
to the Department of Biology
of the Faculty of Arts and Sciences
at the American University of Beirut

Beirut, Lebanon
October 2012

AMERICAN UNIVERSITY OF BEIRUT

COMPARATIVE EFFECTS OF PARTHENOLIDE AND A
SESQUITERPENE LACTONE FROM *COTA PALAESTINA
SUBSP. SYRIACA* ON TUMOR PHENOTYPE OF
MDA-MB-231 BREAST ADENOCARCINOMA CELLS

by
BILAL NASSIB NASR

Approved by:

_____
Dr. Rabih Talhouk, Professor   Advisor
Biology

_____
Dr. Nadine Darwiche, Professor   Member of Committee
Biochemistry and Molecular Genetics

_____
Dr. Najat Saliba, Professor   Member of Committee
Chemistry

_____
Dr. Diana Jaalouk, Assistant Professor   Member of Committee
Biology

Date of thesis defense: October 30, 2012

AMERICAN UNIVERSITY OF BEIRUT

THESIS RELEASE FORM

I, Bilal Nassib Nasr

☐ authorize the American University of Beirut to supply copies of my thesis to libraries or individuals upon request.

☐ do not authorize the American University of Beirut to supply copies of my thesis to libraries or individuals for a period of two years starting with the date of the thesis defense.

_____
Signature

_____
Date

ACKNOWLEDGEMENTS

Ola AL Zein, sadi2atee as I like to call you, you are a Dear friend as well. Thanks for your continuous support, for the nice Dinners "djaj w toum" and for your will to help in all times.

Leila Kamareddine; another sadi2a, thanks a lot for everything.

Isabelle Fakhoury, you are a unique friend. Btw are you still seeking for an RST membership ☺ thanks for all the great times and for your continuous support. I won't forget this: "shay jay shay raye7" :P

Bushra Ajeeb, "BEEB", thanks for your caring my friend. Thanks for providing my dear K100 lamman kan ma2tou3 min el sou2 ;) Wish you the best in your new work.

Tamara Abou matar, RST's adopted grad, thanks a lot. Ma t3azbee l RSTs ☺

Akram Ghantous, we should say Dr. now ☺ and Melody Seikaly, thanks a lot for your help in the experiments and for providing parthenolide.

RST members, "RSTOUMs", YOU ROCK. You are my second family and my friends that I'll never forget. You should never forget these slogans: Team Work is Key, Involve to Evolve, Consistency and others ☺ Dania Al labban, thanks for yourhelp and support. Elia El Habre, "MaMa" ☺, my friend, you are someone I respect a lot. Someone I have enjoyed and still enjoying spending long times with him at 117.You were always there for me, you were always ready to help. I thank you so much. Dana Bazzoun, "2eede l yameen" or "dera3e el 3askaree" ☺ you're another special, dear friend. Thanks for everything my friend. Mike Kareh, "Miko", many thanks for many things you did to me. Take care of Elia ☺ Wish you the best. Hugs and kisses.

Special thanks are due to the best Grads ever, those are the former and current biology Grads. You are really nice people. Be proud of that. Thanks for: Hind Zahr, Nagham Abou Shakra, Caroline Tawk, Elsy Rechdane, Lori Malkhassian, Nivine Naser, Briaa Khalil, Raed Hmadi, Melody Seikaly, Rita Tohme, Lara Kamad, Layla El Mousawe, Carine Jaafar, Emane Abdallah, Farah Abed Ali, Rabiah Hamze, Hadla Hariri, Dayana Hayek, Angela Zaki, Samer Monzer and Ghida Itani. I'm short of words my dear colleagues. Congratulations for those who have graduated and best of luck for the others. I will always visit the Biology to see you and offer any help needed.

Thanks to my friends, Hratch Hassergian, Mark Francis, Talal Nabulsi, Jeremy Arbid, Melissa, Anna and Huda Nassar. Thanks with NO FRONTIERS ☺

Last but not least, I would like to thank my family, my Mom (Hiam), my brothers (Ramy and Salam), my Darling sister (Farah) and my relatives all. None of this would have been possible without your love and patience. Without you this thesis wouldn't have been possible. GOD Bless you all.

This thesis is dedicated to the soul of my father. I'm sure if you were here, you would have been proud of me.

AN ABSTRACT OF THE THESIS OF

Bilal Nassib Nasr   for   Master of Science
Major: Biology

Title: Comparative Effects of Parthenolideand a Sesquiterpene Lactone from *Cota palaestina subsp. syriaca* on Tumor Phenotype of MDA-MB-231 Breast Adenocarcinoma Cells

Sesquiterpene lactones (SLs) constitute a large and a diverse group of biologically active plant compounds that possess anti-inflammatory and antitumor activities. Parthenolide (PTL) is the major SL and the primary compound responsible for the bioactivities of feverfew (*Tanacetum parthenium*). K100, an anti-inflammatory sesquiterpene lactone isolated through bioactive guided fractionation from *cota Palestina subsp.syriaca*,an Eastern Mediterranean endemic plant known in Arabic as 'Bahar ghishai', is analogous to the feverfew-extracted PTL known to inhibit proliferation and apoptosis in many human cancer cell lines.K100 Inhibited Endotoxin(ET)-induced pro-inflammatory markers: IL-6, MMP9 and NO in normal mouse mammary SCp2 Cells. Molecular docking *in silico* of one K100 isomer and DMAPT against several target proteins of PTL predicted that K100 can bind at similar positions as PTL, and with comparable binding affinities. K100 and PTL inhibited the proliferation and prolonged the S phase of the cell cycle of breast adenocarcinoma MDA-MB-231cells in 2D cultures. Non-cytotoxic concentrations of K100 and PTL decreased the proliferation rate of MDA-MB-231 and shifted their morphology from stellate into spherical accompaniedwith a significant increase in the amount of small colonies and a decrease in the amount of large colonies in 3D cultures. Moreover, K100 and PTL decreased cellular motility and invasiveness of MDA-MB-231 cells. Also, K100 and PTLup-regulated the levels of cadherins under 2Dculture conditionsand did not affect the total levels of MMP9 and P65. In summary, these results suggest that K100 exhibit PTL-analogous anti-inflammatory, anti-proliferative and anti-metastatic effects.

CONTENTS

ILLUSTRATIONS

ABBREVIATIONS

/	Per
%	Percent
µg	Micro Gram
µl	Micro Liter
ºC	Degrees Celsius
2D	Two Dimensional
3D	Three Dimensional
ATCC	American Tissue Culture Collection
ATP	Adenosine Tri-Phosphate
bp	base pair
Ca^{2+}	Calcium ion
cAMP	cyclic Adenosine Monophosphate
cGMP	cyclic Guanosine Monophosphate
CMV	Cytomegalovirus
CT	Carboxy Terminus
Cx	Connexin
Cxs	Connexins
DMAPT	Dimethylamino-Parthenolide
DMSO	DimethylSulfOxide
ECM	Extra-Cellular Matrix
EDTA	Ethylene Diamine Tetraacetic Acid
EGFP	Enhanced Green Fluorescent Protein

EHS	Engelbreth-Holm Swarm
ER	Endoplasmic Reticulum
ELISA	Enzyme-Linked ImmunoSorbent Assay
et al.,	et allii (and others)
FBS	Fetal Bovine Serum
FITC	Fluorescein Isothiocyanate
GJ	Gap Junction
GJIC	Gap Junctional Intercellular Communication
H^+	Hydrogen ion
hr	Hour
IP_3	Inositol Tri-Phosphate
IRES	Internal Ribosome Entry Site
JAM	Junctional Adhesion Molecules
Kb	Kilobase
KDa	KiloDalton
MAGI	Membrane-Associated Guanylate kinase Inverted
MAGUK	Membrane Associated Guanylate Kinase
MAPK	Mitogen Activated Protein Kinases
MEC	Mammary Epithelial Cells
min	minute
MMP	Matrix Metalloproteinases
MT	Microtubules
NGS	Normal Goat Serum
NT	Amino Terminus

nm	nanometer
NF-Kb	Nuclear Factor Kappa B
PBS	Phosphate Buffer Saline
PKA	Protein Kinase A
PI3K	Phosphatidylinositol 3-Kinase
PTL	Parthenolide
PVDF	Polyvinylidene Diflouride
SALA	Salgraviolide
SDS	Sodium Dodecylsulfate
Ser	Serine
SL	Sesquiterpene Lactone
Subsp	Subspecies
TBS	Tris-buffered Saline
TGN	Trans-Golgi Network
Thr	Threonine
TJ	Tight Junctions
VEGF	Vascular Endothelial Growth Factor
μ	Micro

CHAPTER I

INTRODUCTION

A. Medicinal Plants and Cancer

Natural products, be it of plant, animal or microorganism origin have been used as part of folk medicine and have made huge contributions to human health through compounds such as aspirin, quinine, morphine and many others (Sharma *et al*., 2010). These products have been and continue to be an essential supplier of the modern pharmacopeia (Demain and Vaishnav, 2011). The anti-cancerous potential of these products was first recognized in 1950s by the US National Cancer Institute (Gordon *et al*., 2005). Now, more than 67% of anticancer drugs owe their origin to natural products and more than 200 of these drugs are in preclinical or clinical trials (Ghantous *et al*., 2010).

Herbal Medicine is the oldest form of medicine worldwide (Efferth, 2010). Biologically active natural products extracted from medicinal plants have been widely recognized as being part of folk medicine for centuries. These products have been used for multiple medicinal practices such as rheumatoid arthritis, toothache, headache, stomachache, menstrual irregularities, arteriosclerosis, hyperlipidemia, inflammatory diseases, immune deficiency, central immune system disorders and cancer (Czyz *et al*., 2010). According to the World Health Organization (WHO) it is estimated that 80% of people rely on herbal medicines for some part of their primary health care globally.

In fact, plants have been an essential source for several anti-tumor agents such as Paclitaxel (Taxol), Navelbine (Vinorelbine), Vinblastine (Velban) and others (Vaishnav and Demain, 2011). Nevertheless, only 5-10% of the 250,000 species of

higher plants that exist on Earth have been investigated so far (Sarker *et al.,* 2009). This will keep plants in the forefront of the struggle against cancer as one of the main sources for new anti-tumor drugs.

B. Plant Secondary Metabolites

1. Definition

Secondary Metabolites are the products of metabolism that are dispensable for development, normal growth, or reproduction of an organism (Vaishnav and Demain, 2010). However, the role of these compounds is enabling the organisms that produce them to fulfill their secondary requirements. They support them to survive interspecies competition, facilitate reproductive processes and provide defensive mechanisms. Known resources for secondary metabolites are plants, bacteria, marine organisms and fungi (Vaishnav and Demain, 2010). In addition to the known primary metabolites such as amino acids, fatty acids and carbohydrates, which occur in all plants and are involved in the primary metabolic processes, plants also synthesize a large variety of compounds, with no apparent function in primary metabolism and thus are called secondary metabolites (Heldt and Heldt, 2012). Plant secondary metabolites (PSMs), also referred to as phytochemicals, constitute a large group of natural products, most of which have no nutritional value (Wink, 2004). However, studies have shown that PSMs have functions that are essential for the plants' fitness. Their main roles include: defense against herbivores, fungi,bacteria and viruses as well as against other plants competing for light, water and nutrients (Wink, 2010). Interestingly, PSMs have been found to have additional medicinal applications besides their known traditional ones. These

applications include cholesterol lowering, antiviral, immunosuppressant and most

importantly antitumor (Vishnav and Demain, 2010).

Despite the great variety of PSMs, the number of basic distinct biosynthesis pathways is

restricted. Precursors are usually the derivatives of the basic metabolic pathways, such

as glycolysis, the Krebs cycle, or the shikimate pathway (Figures 1 & 2) (Wink, 2010).
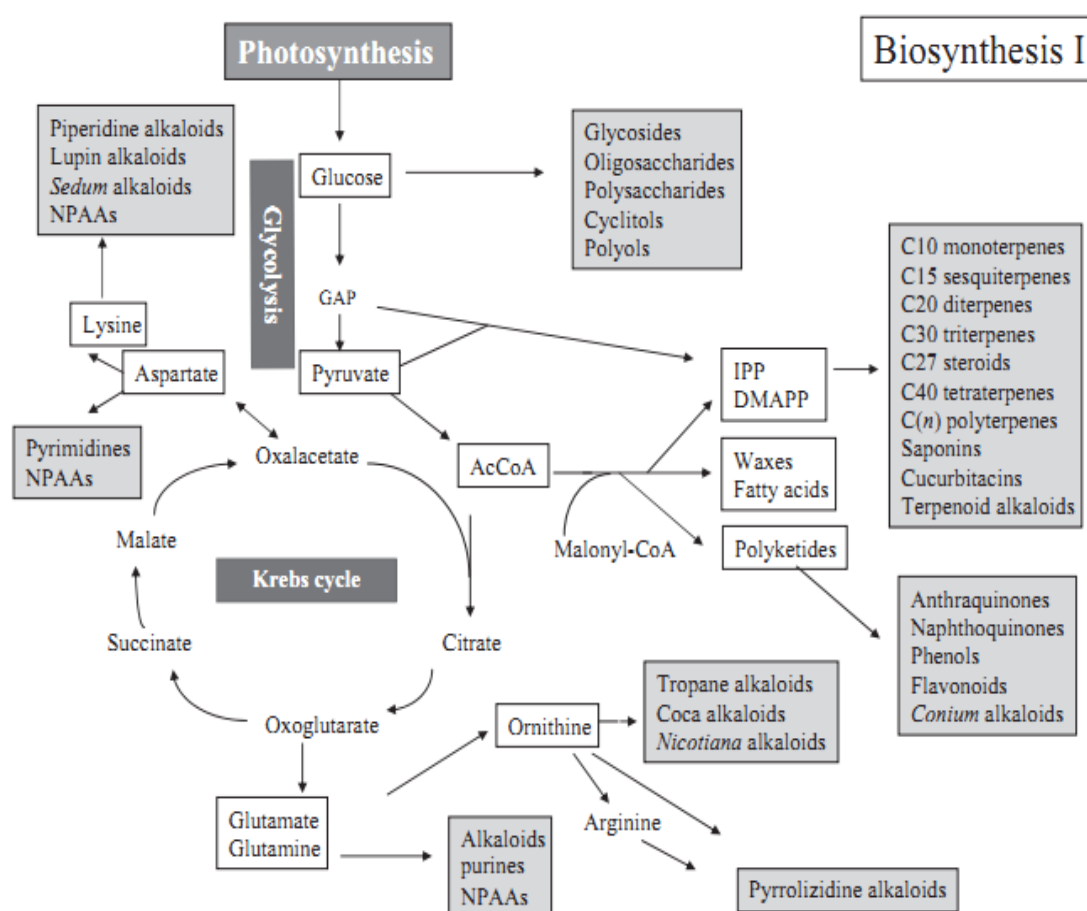
Figure 1. Main Pathways Leading to PSMs. Abbreviations: IPP, isopentenyl diphosphate; DMAPP, dimethyl allyl diphosphate; GAP, glyceraldehyde-3-phosphate; NPAAs, non-protein amino acids; AcCoA, acetyl coenzyme A (Wink, 2010).
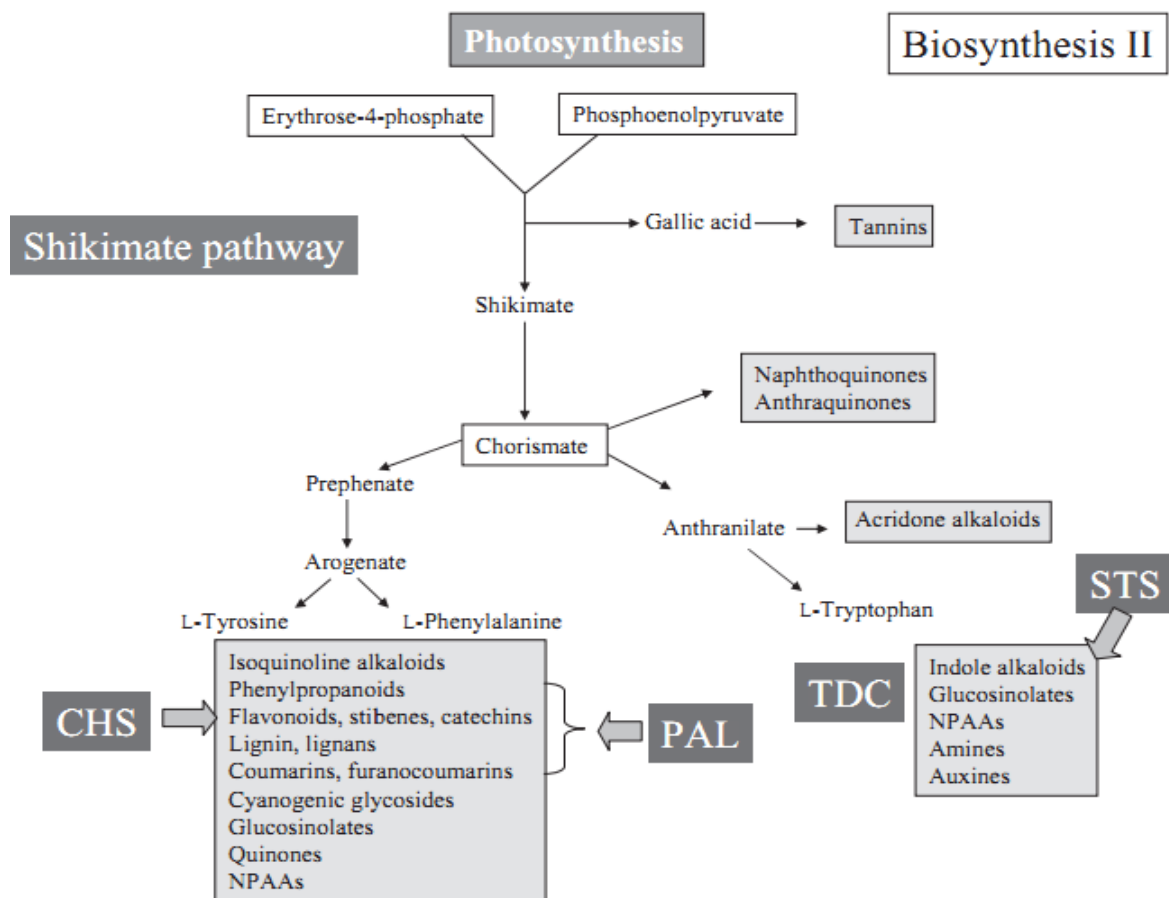
Figure 2. Several Pathways of PSMs derived from precursors (Anthranilate, chorismate and Arogenate) in the shikimate pathway. Abbreviation: NPAAs, non-protein amino acids; PAL, phenylalanine ammonia lyase; TDC, tryptophan decarboxylase; STS, strictosidine synthase; CHS, chalcone synthase (Wink, 2010).

Although PSMs are ubiquitously present plants, their initial site of synthesis is limited to a single organ such as fruits, leaves and roots (Acamovic and Brooker, 2005). Moreover, their production is generally organ-, cell- and often development-specific making their synthesis highly correlated to seasonal, environmental or external stimuli (Wink, 2010).

Classification

Plant secondary metabolites include more than 30,000 compounds and can be divided into four major groups.

a. Acetogenins: These are long-chain aliphatic compounds with more than 35 carbon atoms, ending with a γ-lactone. Their potential medical applications are related to their anti-tumor (e.g. asimicin, bullatacine), insectisidal and anti-bacterial properties (Gurib-Fakhim, 2006).

b. Alkaloids: These are cyclic organic compounds that are mainly formed from amino acids and contain at least one nitrogen atom in a negative oxidation state as constituents of heterocycles (Heldt and Heldt, 2012). They are known for their important role in plant germination and protection and to be plant growth stimulants. Alkaloids have significant pharmaceutical contributions such as quinine as an anti-malarial, morphine as a narcotic analgesics, cholchicine in the treatment of gout and others anti-arrythmic, antispasmodic and anticancer activities (Gurib-Fakhm, 2006).

c. Phenols: These constitute one of the largest groups of PSMs with over 8000 phenolic structures currently known. They have one or more aromatic rings with one or more hydroxyl groups. Phenols are chemically categorized as phenolic acids, flavonoids, tannins, lignans, curcuminoids, stilbenes, coumarins and quinines (Huang and Yi-Zhong, 2010). In addition to their primary antioxidant activity, phenolic compounds display a range of other biological functions which are mainly associated with cancer prevention (Dai and Mumper, 2010). Examples of phenols with anti-cancer activities include strawberry extracts (anthocyanins, kaempferol, quercetin and esters of allergic acid), tea extracts

(epicatechin and epicatechin-3-gallate) and many others. Quercetin is a potent anti-oxidant that has been shown to exert anti-inflammatory, anti-proliferative and pro-apoptotic effects *in vitro* and *in vivo* (Huang and Yi-Zhong, 2010).

d. <u>Terpenoids:</u> Also referred to as terpenes, these compounds represent the largest group of natural compounds. They are made up of two five-carbon building blocks and encompass essential oils (monoterpenes and sesquiterpenes), resins (diterpenes and triterpenes), carotenoids (tetraterpenes), polyterpenes, perfumes (aromatic terpenes), turpentines and saponins (Rabi and Bishayee, 2009). Terpenoids exhibits multiple biological functions including antioxidation, anti-inflammation and anticancer effects. Based on their structure terpenoids are divided into the following groups:

    • Monoterpenes: They are C10 compounds and include a number of compounds (limonene, carveol and carvone) that are implicated in cancer prevention (Wang *et al*. 2005).

    • Sesquiterpenes: They are C15 compounds with a wide range of activities that are mainly attributed to the presence of α-methylene-γ-lactone moiety and epoxides (Gurib-Fakim, 2006). As we are interested in studying the anti-tumorigenic properties of sesquiterpene lactones, this group will be further discussed later.

    • Diterpenes: They are C20 compounds with various biological activities, to which Taxol, the best selling anti-cancer drug, belongs (Rabi and Bishayee, 2009).

    • Triterpenes: They are C30 compounds that have been found to anti-cancer and anti-inflammatory properties. Compounds such as celastrol,

pristemerin, withaferin and ursolic acid were shown effective against several

tumors including breast and prostate (Yang and Ping Duo, 2010).

• Carotenoids: They are C40 compounds. They are responsible for

the orange and yellow colors seen in some vegetables and fruits which are

considered as safe coloring agents for cosmetics and food substances.

Carotenoids such as β-carotene and lycopene are perceived as potential anti-

cancer agents with lycopene being currently in Phase II clinical trials (Yang and

Ping Duo, 2010).

3. Sesquiterpene Lactones

Sesquiterpene lactones represent a large and a diverse group of biologically

active plant products with more than 5000 characterized structural variant (Merfort,

2011). They were identified in several plant families such as Anacardiaceae,

Magnoliaceae, Acanthaceae and Rutaceae *etc*. However, the majority of identified SLs

are derived from the Compositaea (Asterceae) family. They are described as the active

compounds in many medicinal plants and are known to exhibit multiple biological

activities, such as anti-inflammatory, cytotoxic, neurotoxic, allergic, antimicrobial and

antitumor activities (Chaturvedi, 2011). Sesquiterpene lactones are natural terpenoids

with a 15-carbon skeleton formed from three isoprene units. They are categorized on the

basis of their carbocyclic skeletons into four main classes: pseudoguainolides and

guaianalides (5/7-bicyclic compounds); germanocranolides (ten-membered ring);

eudesmanolides (6/6-bicyclic compounds) (Figure 3) (Merfort, 2011). It is generally

believed that the bioactivity of most sequiterpene lactones is based on alkylation of

nucleophiles through their α, β- or α, β, γ-unsaturated carbonyl structures, such as α-

methylene-γ-lactones or α,β-unsaturated cyclopentenones. Therefore, exposed thiol

groups, such as cysteine residues in proteins, are considered the major targets of SLs, thereby interfering with a variety of biological functions (Regina *et al*., 2012). However, the activity of SLs can be influenced by other factors such as the number and the reactivity of alkylating elements, lipophilicity and molecular geometry (Ghantous *et al*. 2010).

| germacranolide | eudesmanolides | guianolides | pseudoguaianolides |
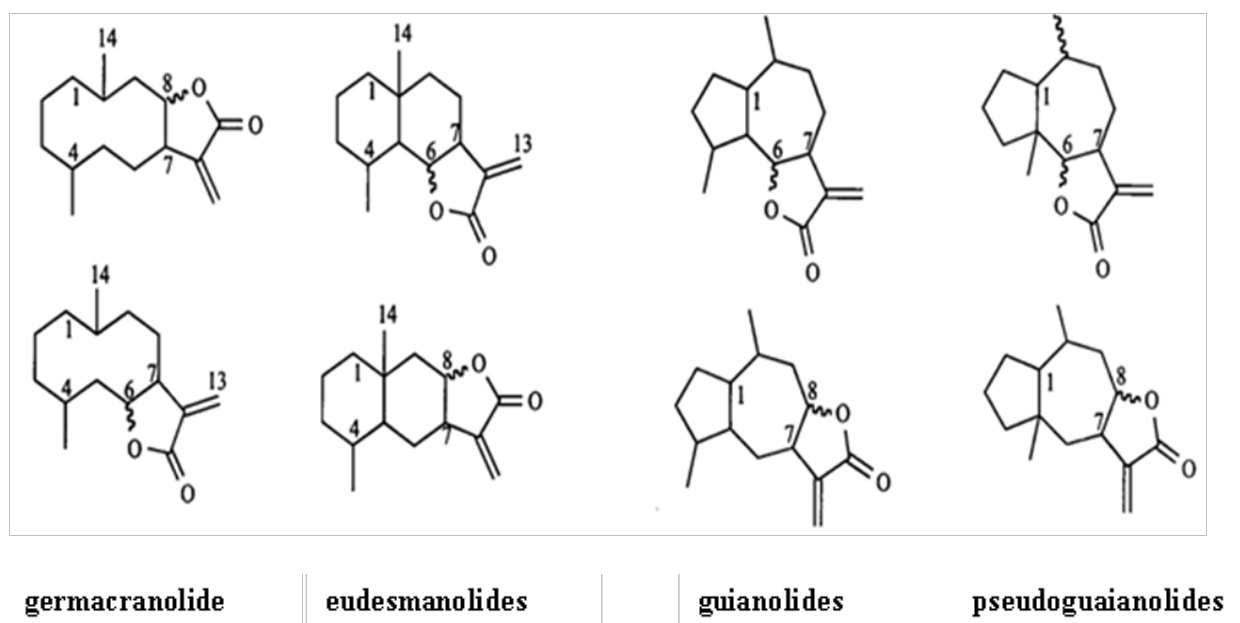
Figure 3. Chemical structure of the major SLs' groups. All SLs contain an α-methylene-γ-lactone ring either cis- or trans- fused to the C6-C7 or C8-C7 position of the carboxylic skeleton The terms cis or trans refer to the orientation of the 5- or 7-membered rings situated on opposite sides of the bond linking C1 and C5 (Merfort, 2011).

Recently, the anti-tumor activities of different SLs have gained a great deal of interest and extensive research has been conducted to study the molecular mechanisms of their anticancer effects as well as their potential use as chemotherapeutic and chemopreventive agents. SLs in cancer clinical trials are artemisinin from *Artemisia annua* L, thapsigargin from *Thapsia* (Apiaceae) and parthenolide from *Tanacetum parthenum* (feverfew) and their synthetic derivatives. Reacting covalently with

8

biological nucleophiles, especially with cysteine sulfhydryl groups of proteins, thereby affecting a variety of cellular functions in cells including the functions of sarco/endoplasmic reticulum (ER) calcium ATPase (SERCA) pump, particular proteases secreted by cancer cells, high iron content and cell surface transferrin receptors, nuclear factor- kB (NF- kB) signaling, MDM2 degradation, p53 activation, angiogenesis, metastasis, and epigenetic mechanisms. Their pleiotropic actions have rendered these agents effective against several tumor cells (Figure 4) (Vasas and Hohmann, 2010). In addition to these key factors, several SLs were shown to upregulate or downregulate c-Jun-N-terminal kinase (JNK) and mitogen-activated protein kinase (MAPK) and interfere with signal transducer and activator of transcription 3 (STAT3), there by disrupting cell cycle progression (Hsu *et al.* 2009; Nakshatri e*t al.*, 2004). One SL, artemisinin, has been reported to inhibit the proliferation and induce cell cycle arrest at G1 phase in LNCaP (lymph node carcinoma of the prostate) human prostate cancer cells (Willoughby *et al*., 2009). Moreover, several studies have shed the light on the ability of SLs to promote cell differentiation, an essential process in oncogenesis. For example, Costunolide has been reported to promote cell differentiation in human leukemia derived HL60 cells and inhibit endothelial cells angiogenesis (Jeonga *et al*., 2002; Choi *et al.,* 2002). Recently, Costunolide was shown to inhibit the growth and induce apoptosis through extrinsic pathway in MDA-MB-231 breast cancer cells (Choi *et al*., 2012). All these data and a lot of other research studies conducted on SLs have proven that these compounds could also play a valuable role as lead structures to new therapeutic agents.
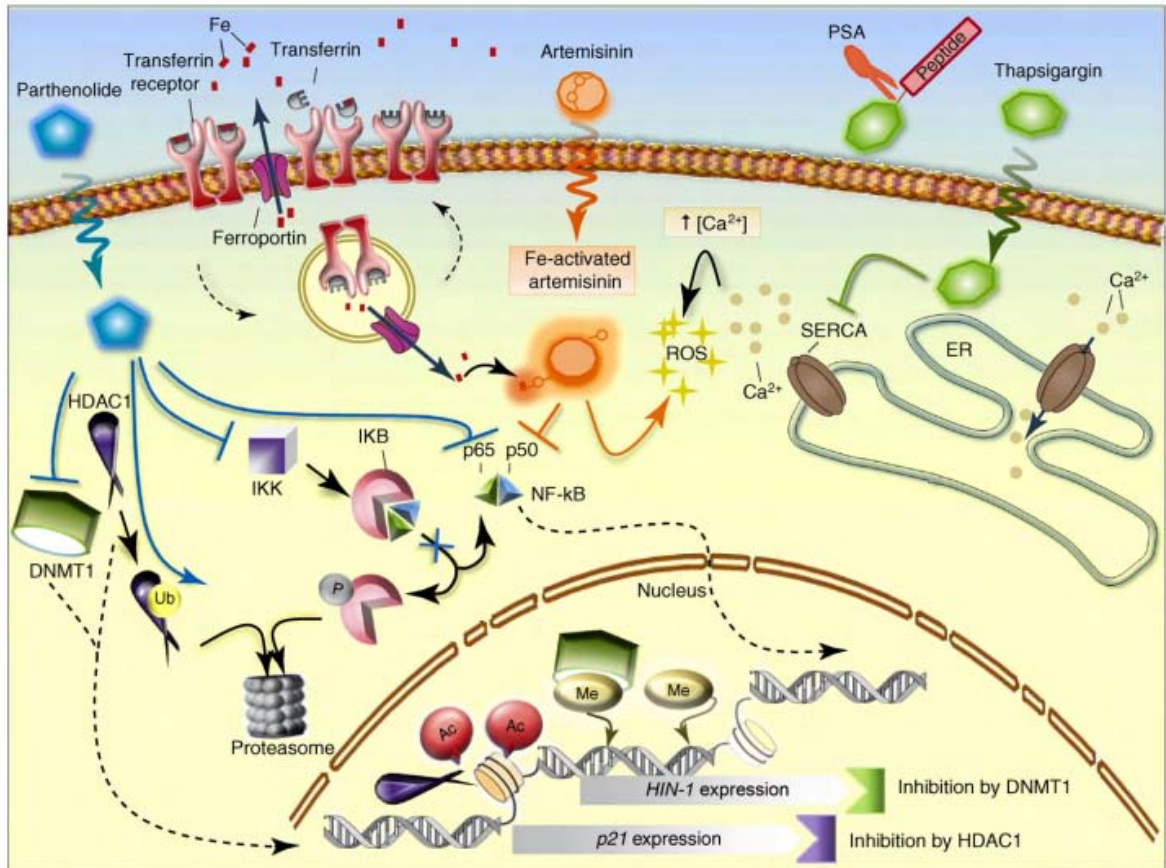
Figure 4. Sesquiterpene lactones target several pathways in tumor and cancer stem cells. There are several sesquiterpene lactones in clinical trials including or deriving from thapsigargin, artemisinin and parthenolide. Sesquiterpene lactones diffuse through the plasma membrane and target the SERCA pump, high iron content and cell surface transferrin receptors, NF- kB signaling, and epigenetic mechanisms. Thapsigargin can diffuse into the SERCA pump blocking its ability to transfer Ca2+ from the cytosol into the ER. High cytosolic Ca2+ concentrations lead to the generation of ROS and subsequent cell death. Many cancers have high intracellular Fe content and elevated levels of transferrin receptors. Cytosolic Fe binds to artemisinin's endoperoxide bridge, causing its activation and the generation of toxic ROS. Parthenolide directly inhibits DNMT1 and causes ubiquitin-mediated proteasomal degradation of HDAC1, leading to express ion of HIN-1 and p21, respectively. Parthenolide directly inhibits the NF-k B p65 subunit and the IKK complex preventing IKK-mediated phosphorylation and proteasomal degradation of Ik B. Artemisinin also inhibits NF- k B activity. Abbreviations: Ac, acetyl group; DNMT1, DNA methyl transferase; ER, sarcoplasmic/endoplasmic reticulum; HDAC1, histone deacetylase 1; IKK, IkB kinase; IkB, inhibitor of NF- kB; PSA, prostate-specific antigen; Me, methyl group; NF-k B, nuclear factor- kB; ROS, reactive oxygen species; SERCA, ER calcium ATPase; Ub, ubiquitin. Dashed and solid lines indicate translocation and activation, respectively (Ghantous *et al*., 2010).

C. *Cota Palaestina* and K100

The genus Cota J. Gay belongs to the tribe Anthemideae, one of the largest tribes of the sunflower family (Asteraceae = Compositae), including approximately 110 genera and 1800 species. Historically, Cota was considered a subgenus of the closely related genus Anthemis L. known for its medicinal properties (De Costa et al., 2005). Hence, most of the literature on the medicinal properties and biological activities of Cota spp. treats these species as members of Anthemis. Today, Cota is recognized as an independent genus by Greuter *et al.* (2003), Oberprieler *et al.* (2007, 2009), and Lo Presti *et al.* (2010). Cota palaestina Kotschy (= Anthemis palaestina ssp. syriaca (Bornm.) R. Fern.) is an Eastern Mediterranean endemic known in Arabic as 'Bahar ghishai' (Euro+Med PlantBase). It flowers in April and May (Figure 5) (Post and Dinsmore, 1932).

The chemical composition and biological activities of Cota palaestina remain poorly investigated. The water extract of its aerial parts were previously screened for antimicrobial and anti-inflammatory activities, showing efficacious inhibitory effects in both, yet its chemical constituents were not identified (Barbour *et al.*, 2004; Talhouk *et al.*, 2007). In fact, most Anthemis species that have been studied are known to contain SLs, and in most of these species, the identified SLs belong to three major groups: germacranolides, eudesmanolides, and guaianolides (Çelik *et al.*, 2005; Da Costa *et al.*, 2005). Over the centuries, Anthemis species were widely exploited in folk medicine due to the therapeutic effects they exhibited, including: sedative or anti-inflammatory, antimutagenic or antigenotoxic, antiphlogestic, antiepileptic, mitogenic, spasmolytic, anxiolytic, antimycobacterial, insectisidal and antimicrobial agents (Teixeira da Silva *et al.*, 2004).

Figure 5. *C. palaestina* (Compositeae) is a plant endemic to Lebanon with claimed medicinal value (Arabic name; Bahar ghishai). The plant grows in Dayr-ul-Ahmar to Aynata region at elevations of 1200 – 1800 m above sea level, respectively. It is also reported in Anti-Lebanon Mountain range above Ayn-Burday at 1250-1300 m. The plant is glabrous, and branching from neck; its stems are erect, and sparingly branched. The leaves are oblong in outline; its peduncles are long not thickened. The flowering season is during the months of April and May. A specimen is deposited at the herbarium of the American University of Beirut, Beirut, Lebanon (photos courtesy of Khaled Sleem 2008, Landscape Design and Ecosystem Management, Faculty of Agriculture and Food Science, American University of Beirut. Beirut, Lebanon). *From: Flora of Syria, Palestine, and Sinai. George Post* (2nd Edition, John Edward Dinsmore, 1933).

K100, as referred to in our studies is the bioactive molecule extracted from this plant, was identified through bioactive-guided fractionation using column chromatography and spectroscopic techniques. K100 reduced IL-6 production by Endotoxin (ET)-treated mammary epithelial cells (SCp2), a culture system previously reported effective in screening for anti-inflammatory bioactive molecules (Talhouk and Saliba *et al*., unpublished data). Spectroscopic data confirmed that the germacranolide 1β,10α-Epoxy-6α-hydroxy-1,10H-inunolide is isolated and identified as an anti-inflammatory compound for the first time in Cota palaestina (Figure 6). This compound was previously identified in Mikania goyazensis. The spectroscopic data are in agreement with the reported literature (Bohlmann et al., 1982). However, we additionally reported the position of the OH hydrogen in 1H NMR. Bohlmann *et al.*, (1982) reported another isomer structure to 1β,10α-Epoxy-6α-hydroxy-1,10H-inunolide, but with the lactone ring junction attached trans instead of cis. Also, Konstantinopoulou *et al.*, (2003) reported another isomer where the epoxide moiety's stereochemistry is inverted relative to 1β,10α-Epoxy-6α-hydroxy-1,10H-inunolide. However, no biological activities were attributed to any of these structures. K100 has structural similarities to parthenoloide (PTL), the major sesquiterpene lactone (SL) extracted from the plant Tanacetum parthenium (feverfew). K100 bear similar functional goups to those found in PTL, namely an exocyclic α-methylene-γ-lactone ring and an epoxide moiety. The potent anti-inflammatory action of K100 may be attributed to the presence of three chemical groups: a) an exocyclic α-methylene-γ-lactone, b) a hydroxyl (OH) group adjacent to the α-methylene and c) an epoxide. The OH group decreases lipophilicity and increases the solubility of the molecule and its location next to the α-methylene was found to enhance the rate of cysteine addition, thereby increasing activity. Moreover,

the presence of the epoxide moiety along with an exocyclic α-methylene-γ-lactone in the same compound is assumed to maximize its biological activity.
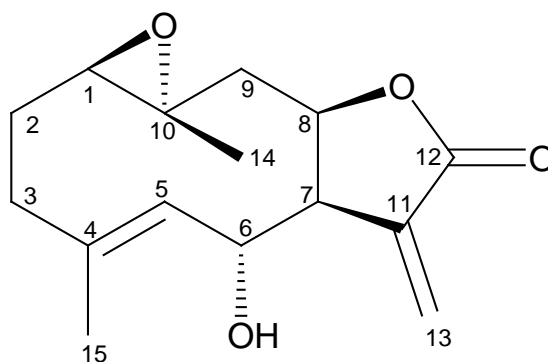
1β,10α-Epoxy-6α-hydroxy-1,10H-inunolide
(K100)

Figure 6.Structure of the anti-inflammatory component "K100", the germacranolide 1β,10α-Epoxy-6α-hydroxy-1,10H-inunolide, in *C. palaestina* (Talhouk and Saliba *et al*., unpublished data).

D. *Tanacetum parthenium* and Parthenolide

Tanacetum parthenium (L.) Sch. Bip., commonly known as feverfew, belongs to the family Astraceae (the "Daisy" family and previously known as the compositaea family). This large family includes some 25,000 species and 1400 genera and is found in most ecosystems except for Antarctica (Gurib-Fkim, 2006). Feverfew is a daisy-like perennial plant with a very similar appearance to chamomile (Figure 7). Feverfew is originally a native of Europe's Balkan mountains and now grows in Australia, Japan, China, North Africa, North and South America, and Europe. This plant contains diverse natural products including sesquiterpene lactones, flavonoid glycosides, pineses and other compounds. Feverfew is a popular medicinal plant that traditionally has been used for the treatment of migraine headaches, fever, and rheumatoid arthritis (Kemper, 1999).

14

Figure 7. Feverfew (*Tanacetum parthenium*): whole plant (a), flower (b), and feathery leaves (c).(Pareek *et al.*, 2011).

Parthenolide (PTL) is the major SL and the primary bioactive compound in feverfew (Figure 8). PTL has been shown to have anti-microbial, anti-inflammatory as well as anticancer activities. PTL anti-inflammatory activities are mainly attributed to the inhibition of NF-kB (Hehner *et al.*, 1999). Nevertheless, NF-kB, a ubiquitous transcription factor responsible for the regulation of many essential cellular functions including apoptosis, cell proliferation, and differentiation has been shown to be constitutively active in various tumors including breast cancer. Consequently, NF-kB inhibition has been of great interest as one of the main strategies in anticancer therapy (Pajak *et al.*, 2008). Moreover, a more soluble and orally bioavailable PTL analogue, di-methyl-amino-PTL (DMAPT), has similar effects to those of PTL in vitro as well as in vivo and is currently in Phase I clinical trials against acute myeloid leukemia (AML) and other blood and lymph node cancers (Guzman *et al.*, 2009). In fact, recent work has shown that PTL inhibits cellular proliferation, promotes cell differentiation and induces apoptosis mainly by binding to and inhibiting the function of the nuclear transcription factor-kappa B (NF-kB), janus kinase (JAK), signal transducer and activator of transcription (STAT) pathway and tumor necrosis factor (TNFα) signaling pathways (Pajak *et al.*, 2008).
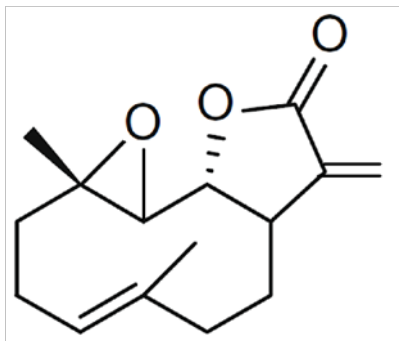
Parthenolide (PTL)

Figure 8. Chemical structure of sesquiterpene lactone parthenolide.A naturally occurring phytochemical in Tanacetum parthenium with multiple medicinal properties.

For example, PTL was shown to be capable of suppressing the proliferation and inducing apoptosis in many human cancer cells in vitro, such as hepatoma, human lung carcinoma (A549), human medulloblastoma (TE671), cholangiocarcinoma, colorectal, pancreatic and breast cancers (MDA-MB231 and MCF-7) (Zhang *et al.* 2004; Parada *et al.* 2007; Kim *et al.* 2005; Pajak *et al.*, 2008). Furthermore, other reports have shown that PTL can specifically eradicate malignant cells, such action was addressed by Guzman *et al.* 2009 who showed that PTL preferentially targets leukemia stem cells while sparing normal hematopoetic stem cells.

Added to its aforementioned anti-proliferative effects against various tumor cell lines, PTL was shown to sensitize several cancer cells to anti-tumor agents (Liu *et al.* 2010). Furthermore, PTL was shown to inhibit migration and invasive ability of pancreatic cell line BxPC-3 (Liu *et al.* 2010). Moreover, PTL has been reported to cause cell cycle progression arrest at the G2/M check point in the sarcomatoid hepatocellular carcinoma cell line (SH-J1) and at the G1 phase in the human 5637 bladder cancer cells (Cheng *et al*. 2011).

16

E. Mesenchymal-Epithelial Transition: Focus on Breast Cancer

Epithelial and mesenchymal cells contribute to the structure and function of developing organs during many stages of embryonic development. Nevertheless, these phenotypes are not always permanent and instead epithelial and mesenchymal cells tend to convert between these two phenotypes under certain conditions. These processes, named Epithelial-Mesenchymal Transition (EMT), and its reverse Mesenchymal-Epithelial Transition (MET), represent a stepwise cycle of epithelial plasticity thereby allowing for normal tissue remodeling and diversification during development. In fact, EMT and the reverse process MET, have both been extensively studied in mammalian development, where the switch between the two phenotypes was found critical for numerous embryonic events and developing organs including gastrulation, neural crest formation, palatogenesis, heart valve formation, nephrogenesis and myogenesis. In addition, this epithelial-mesenchymal plasticity is essential to many aspects of mammary gland development, particularly during branching morphogenesis. Also, it has been shown to be a key process in breast cancer progression (Godde *et al*., 2010).

EMT is a biological process whereby a polarized epithelial cell, which under normal conditions interacts with basement membrane via its basal surface, goes through multiple biochemical changes that enable it to assume a mesenchymal cell phenotype. EMT encompasses loss of epithelial characteristics, including apical-basal polarity and specialized cell-cell junctions and gain of mesenchymal properties, such as front-rear polarity associated with weak cell-cell contacts, increased motility, resistance to apoptosis and invasiveness (Godde *et al*., 2010). Upon completion of the EMT, which is signaled by the degradation of the underlying basement membrane, a mesenchymal cell is formed that can migrate away from the epithelial layer in which it originated (Kalluri

17

et al., 2003).

Transitions through cell polarity states represent a central feature of epithelial plasticity. In fact, EMT starts with the loss of apical-basal polarity as tight junctions (TJs) dissolve allowing the intermingling of apical and basolateral membrane proteins (Figure 9). Then other cellular junctions, including adherens junctions (AJs) and gap junctions (GJs), begin to disassemble and the underlying basement membrane is degraded (Townsend *et al.*, 2008; Peinado *et al.*, 2004).
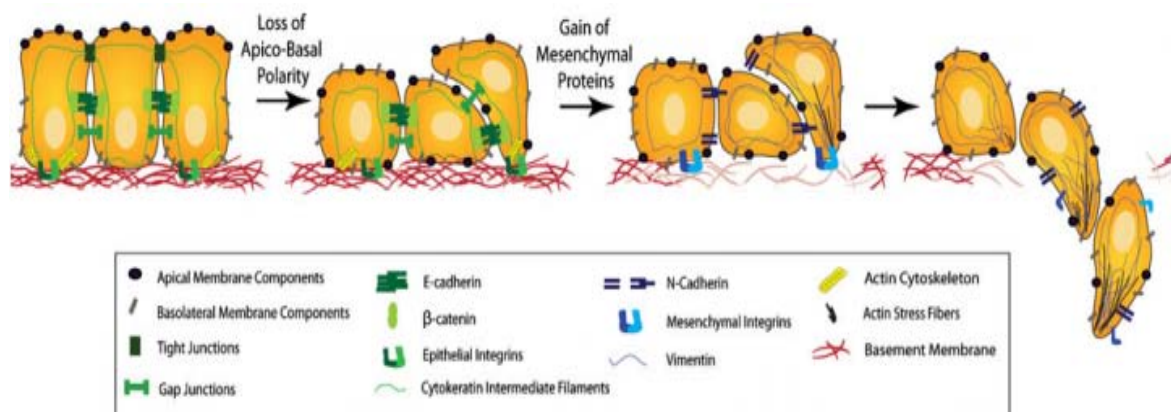
Figure 9. EMT begins by loss of apico-basal polarity by epithelial cells. TJs, AJs and GJs disassemble, and cell surface proteins such as epithelial specific integrins and E-cadherin (green) are replaced by N-cadherin (blue). Stress fibers accumulate at areas of cell protrusions, and cytokeratins are replaced by vimentin. Meanwhile, the underlying basement membrane is degraded resulting in the invasion of the cells to the surrounding stroma (Micalizzi *et al.*, 2010).

EMT occurs in three distinct biological settings and is now classified into three subtypes based on the functional consequences they carry and the biological context in which they occur. Type 1 EMT or developmental EMT occurs during development and accounts for the complex tissue types and organization present in metazoans. Type 2 EMT is associated with tissue regeneration and organ fibrosis. Type 3 EMT or

oncogenic EMT is the one occurring in carcinoma cells, and is associated with tumor

progression and metastasis (Figure 10) (Drasin *et al.*, 2011).
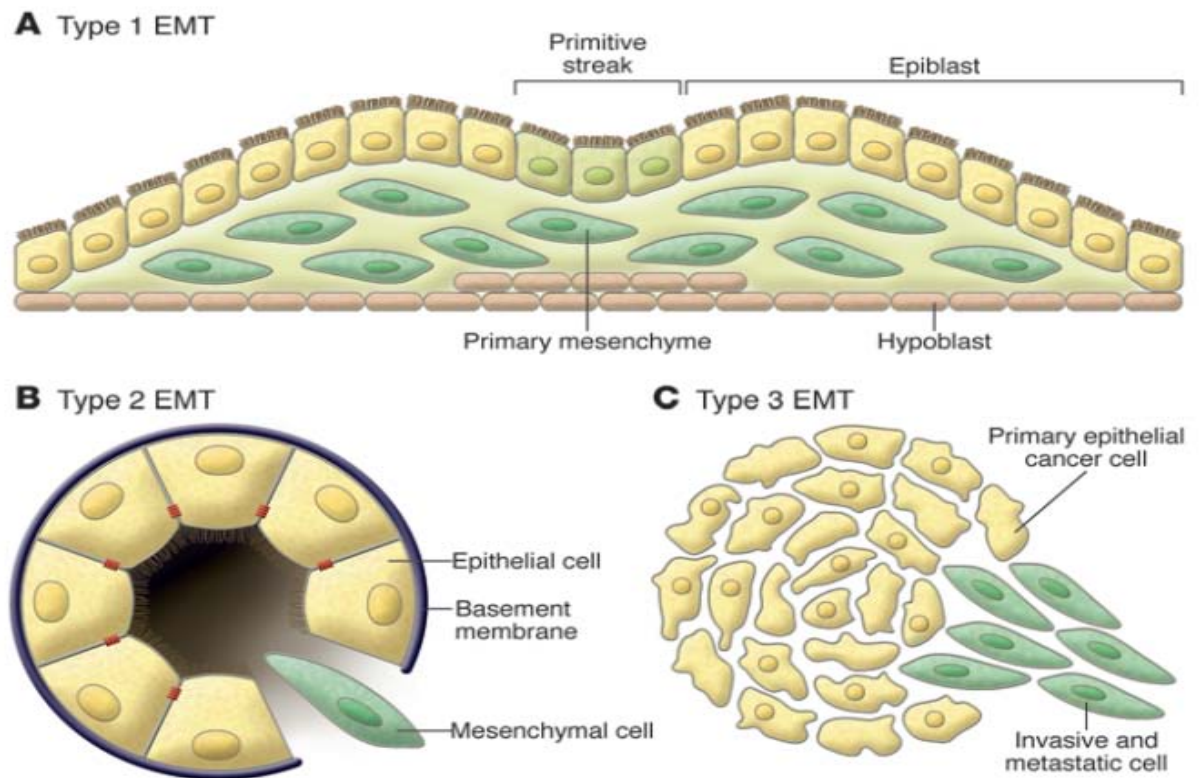
Figure 10. Different types of EMT. (A) Type 1 EMT is associated with implantation and embryonic gastrulation resulting in the formation of the endoderm, mesoderm and mobile neural crest cells. (B) Type 2 EMT involved in inflammation and tissue fibrosis. (C) Type 3 EMT enabling invasion and metastasis of cancer cells (Kalluri *et al.*, 2009).

Oncogenic EMTs are not the same as developmental EMTs. Instead, they

should be perceived as partial EMT, whereby carcinoma cells gain characteristics of

mesenchymal cells; however, they may not totally lose their epithelial characteristics

(Drasin *et al.*, 2011). In fact, EMT as well as MET are recognized as critical events for

metastasis of carcinomas including breast carcinoma. Breast cancer is the most common

malignant tumour diagnosed worldwide where it occupies the second place for cancer-

related deaths in women. More than 90% of breast cancer-related death are not caused by the primary tumors, but rather by their metastasis at distant sites. As yet, there is no cure for metastatic breast cancer. Therefore studying the molecular mechanisms of metastasis and unraveling therapeutic targets to prevent the spread of cancer may represent a breakthrough in the fight against cancer (Gunasinghe *et al*., 2012). Surprisingly, recent studies have shown that some metastases of a number of carcinomas including breast carcinoma, prostate cancer, ovarian cancer, colorectal cancer and hepatic carcinoma share similar epithelial nature to their primary tumors which is inconsistent with the theory of EMT. In order to resolve this contradiction, a MET process was proposed as a part of the process of metastatic tumor formation. As such, it is thought that EMT is needed for the initial transformation from benign to invasive carcinoma, whereas MET is crucial for the later stages of metastasis allowing the formation of secondary tumors at the site of metastatic colonization (Figure 11) (Yao *et al.,* 2011).

The factors involved in the initiation of metastasis have been the focus of extensive research in the past; however, only few studies have examined the formation of secondary tumors. Nonetheless, the role of MET in metastasis has been gradually recognized, and more studies on the mechanism of MET are done. In fact, despite the large number of in vitro and in vivo studies, evidence in support of MET from human specimens is rare because clinically detectable metastases are past the micrometastatic stage at which this transition occurs (Chao *et al*., 2012).
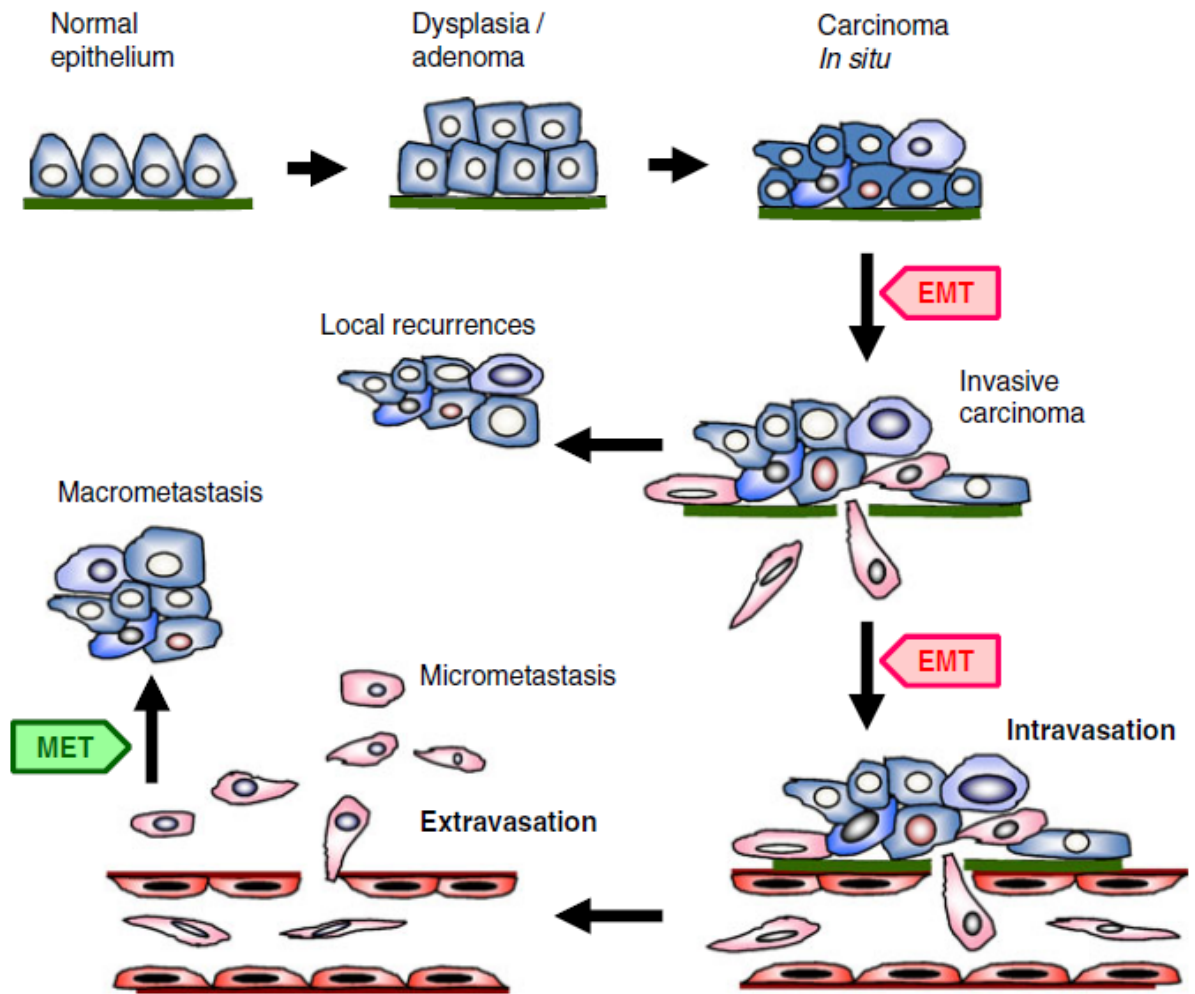
Figure 11. EMT *versus* MET processes that are hypothesized to take place in breast cancer progression. Normal epithelial cells go through a series of transformational changes to become malignant. Proliferation of malignant cells results in invasive carcinoma. Part of these cells invades local tissue forming local recurrences while other part of cells undergo EMT and intravasates into the surrounding blood vessels. Circulating tumor cells may remain in the circulation or extravasate at distant site. Surviving extravasated cells could remain indolent as small micrometastasis or reestablish colonies giving rise to secondary tumors via a reverse mechanism, MET (Devika *et al*., 2012).

Several research groups have worked on elucidating the causes and effects of MET on breast cancer where numerous mediators of MET have been discovered including transcription factors, signaling molecules and microRNAs (miRNAs). Among the several factors implicated in MET during mammary tumor progression, E-cadherin plays a critical role. E-cadherin, an important transmembrane protein that is localized to

21

the adherens junctions and basolateral plasma membrane, represents the best characterized molecular marker expressed in epithelial cells. Recently, it was shown that ectopic expression of E-cadherin in MDA-MB-231 cells resulted in morphological and functional reversion of the epithelial phenotype. Moreover, E-cadherin re-expression was reported at distant metastatic tumors originating from E-cadherin-low or E-cadherin-negative primary tumors. Also, a strong E-cadherin expression was reported in more than 50% of brain, liver and lung metastasis originating from infiltrating ductal carcinoma of the breast. These data suggests that re-expression of E-cadherin is not only an essential hallmark of MET but may be also an important inducer of it (Caho et al., 2010). In addition to E-cadherin, other important factors include the epidermal growth factor receptor (EGFR) and human epidermal growth factor receptor-2 (HER2) which belong to the receptor tyrosine kinase family and are known to play an important role in normal development. These factors are constitutively over expressed in malignant tumors and are thought to contribute to tumor progression. Interestingly, in vitro inhibition of autocrine EGFR signaling increased E-cadherin expression and cell-cell heterotypic adhesion (Yao *et al*., 2011). Moreover, the EGFR tyrosine kinase inhibitor erlotinib was shown to inhibit invasiveness and cell motility and revert the mesenchymal phenotype of inflammatory breast cancer cells to epithelial phenotype in a three-dimensional culture where E-cadherin upregulation and vimentin down-regulation were induced and β-catenin was recovered in the cell membrane (Zhang *et al*., 2009).

On the other hand, several transcription factors were found to be associated with the repression of E-cadherin and are suppressed during MET including zinc finger proteins of the Twist and Snail families. Also, downregulation of ZEB1, Slug, Snail, SMA or Twist is usually induced during MET (Yao *et al*., 2011). Recently, a study has

shown that progesterone (P4) can regulate the expression of Snail and other EMT-relevant proteins in human breast cancer cell line MB468 and induce cell morphological reversion from mesenchymal to epithelial phenotypes via membrane progesterone receptor α (MPR α) (Zuo *et al*., 2010). Furthermore, it was found that decreasing the expression of ZEB1 and ZEB2 via shRNA in mouse mammary gland cells was capable of upregulating the expression of epithelial proteins including E-cadherin and reestablishing epithelial features (Das *et al*., 2009).

In addition to transcription factors, several microRNAs have been shown to be implicated in the induction of MET. MicroRNAs represent a class of small non-coding RNAs that post transcriptionally regulate gene expression and play important roles in many physiological and pathological processes including tumor development. The two microRNA families, miRNA 200 and miRNA 205 are expressed in well-differentiated epithelial breast carcinoma cells and down regulated in invasive and generally mesenchymal breast carcinoma cells. miRNA 200 family was shown to target the transcriptional repressors of E-cadherin thereby inhibiting the initial step of metastasis and EMT by maintaining the epithelial phenotype. Interestingly, among four isogenic mouse breast cancer cell lines (67NR, I68FARN, 4TO7, and 4T1) only 4T1 cells which had high levels of miR-200 family miRNAs and E-cadherin were able to form macroscopic metastasis when implanted into mammary fat pads. Moreover, overexpression of miR-200 in 4TO7 cells allowed them to metastasize to lung and liver (Dykxhoom *et al*., 2009; Hurteau *et al*., 2007). All these finding show that miR-200 family can induce MET and may play a critical role in metastasis formation.

F. Studies on MDA-MB-231 Cells

a. MDA-MB-231 as a model of Breast Cancer

Breast cancer is not a single disease, but rather a collection of diseases having distinct histopathological features, genetic and genomic variability and various prognostic outcomes. Therefore, the major challenge in advancing our knowledge of the biology of breast cancer is the availability of experimental model systems that mirror the several forms of this disease. As a result of this complexity and heterogeneity, no single model is expected to recapitulate all aspects of the disease. As such, several experimental models have been used to investigate the initiation and the progression of breast cancer including human breast cancer cell lines (BCC), xenografts and genetically engineered mice. Despite the several questions raised over how representative immortalized cell lines are of human breast cancer, these remain an efficient experimental tool when used in the proper way (Holliday and Speirs, 2011). In fact, there is a small number of breast cancer cell lines and only a few of them have been extensively studied. Nevertheless, a significant part of our understanding of breast carcinomas is based on in vivo and in vitro studies performed on these cell lines. These cell lines offer an unlimited supply of homogenuous cell population that is capable of self replication, free of contaminating stromal cells, and can be easliy cultured in standard cell culture medium (Lacroix and Leclercq, 2004). Recently, studies investigating the power of BCC lines as model systems through comparing the gene expresson profile and genomic alterations of multiple BCC lines have shown that a panel of cell lines rather than a a single cell reflect the heterogeneity observed in primary breast cancers (Vargo-Gogola and Rosen, 2007).

A large number of BCC lines were established in the late 1970s. A medline (http://www.ncbi.nlm.nih.gov/PubMed/) based survey has shown that very few BCC lines, namely MDA-MB-231, MCF-7 and T-47D, account for more than two-thirds of all abstracts reporting studies on mentioned BCC lines (Lacroix and Leclercq, 2004).

The MDA-MB-231 cell line is an estrogen receptor alpha (ERα)-negative human breast cancer cell line (liu *et al.*, 2003). It was derived from a metastatic adenocarcinoma of the mammary gland of a 51-year-old Caucasian woman, according to the data sheet of the American Type Culture Collection (ATCC). It is a highly aggressive, invasive and poorly differentiated human breast cancer cell line. Thus this cell line is more considered as a representative of aggressive and metastatic cancers rather than the primary tumors (Burdall *et al.*, 2003). These cells are among the most commonly used breast cancer cell lines in medical research laboratories. In addition to their use in common two dimensional (2D) culture systems, MDA-MB-231 cells have also been used in three dimensional (3D) culture systems to investigate the critical signaling pathways that regulate breast tumor biology. Actually, 3D in vitro models are thought to span the gap between 2D and in vivo animal models thereby increasing the physiological significance of cell-based assays. These 3D model systems are thought to better mimic the in vivo tumor environment in terms of oxygen gradients, cell-cell interactions, matrix deposition, cellular heterogeneity, gene expression profiles and drug sensistivity (Vinci *et al.*, 2012). Moreover, 3D models have provided valuable insights into the contributions of molecular factors towards breast epithelial cell behaviors and breast cancer initiation and progression. In fact, 3D epithelial culture systems are perceived as a valuable tool for modelling cancer genes and pathways in a structurally appropriate context (Vargo-Gogola and Rosen, 2007). Recently, a minitumor 3D model

consisting of endothelial cells and fibroblasts in coculture with MDA-MB-23A cells was established for the study of breast tumor angiogenesis in vitro. This model is believed to be an ideal model for high content studies of gene function in individual cell types, allowing for investigating their roles in cell-cell interactions (de Sampaio *et al.*, 2012). In addition, growing BCC lines including MDA-MB-231 cells as xenografts has been proved as a powerful model system for the in vivo analysis through providing powerful tools to investigate various aspects of breast cancer biology. Xenografts of breast tumors have been used to investigate many facets of breast cancer including the genetic alterations involved in tumor initiation and growth, the role of microenviroment (tumor cell-extracellular matrix interactions, inflammation and angiogenesis), and the multistage process of metastasis (Heppner *et al.*, 2000). For example, MDA-MB-231 cells were used in an intravenous experimental metastasis assay to identify a set of genes that marks and mediates breast cancer metastasis to the lungs (Minn *et al.*, 2005). In another study, MDA-MB-231 cells were injected into the mouse mammary fat pad where they form primary tumors and then metastasize into the liver of the mice. This model has allowed for a genome-wide analysis of gene expression profiles of both tumor cells and the associated stromal tissue which is critical in understanding tumor biology (Iorns *et al.*, 2012).

b. Reversion of Phenotype Studies

Studies on MDA-MB-231 cells have clearly shown that these cells bear a mesenchymal-like phynotype that allows the cells to be a highly metastatic breast cancer cell line. Therefore targeting this phenotype through establishing potential anticancer drugs will represent an important step in the control of the metastatic potency and growth of breast cancer cells and other malignancies. In fact several studies have

described the reversion of mesenchymal phenotype process using various human breast cancer models. A recent study by Chao and colleagues have shown that ectopic expression of full length E-cadherin as well as coculture of MDA-MB-231 cells with liver parenchyma cells or following metastasis to the lungs were able to restore a more epithelial morphology of MDA-MB-231 cells. The nature of these signals driving this reversion are not yet known and are believed to be complex. However these results clearly point toward an essential role for the tumor microenviroment in this observed reversion (Chao *et al.*, 2010). In another study the functions of Src homology phosphotyrosyl phosphatase 2 (SHP2), which is an essential transducer of mitogenic and cell survival signaling in the epidermal growth factor receptor (EGFR) signaling pathway, has been studied in breast cancer cell lines. Inhibition of SHP2 resulted in a suppression of EGF-induced activation of Ras extracellular signal- regulated kinase (ERK) and phosphatidylinositol 3-kinase (PI3K)-Akt signaling, induced epithelial cell morphology and resulted in a reversion to a normal breast epithelial phenotype. SHP2 inhibition has led to an upregulation of E-cadherin and downregulation of vimentin and fibronectin. These results show an important role of SHP2 in the mesenchymal to epithelial phenotype reversion in breast cancer (Zhou and Agazie, 2008).

Moreover, studying the role of bone morphogenetic protein 7 (BMP7), a member of the BMP family, in the development and treatment of bone metastasis from breast cancer has revealed interesting results correlated with breast tumor phenotype reversion. It was shown that tumorigenicity and invasive behavior of breast cancer cell lines are inversely related to BMP7 expression. Interestingly, BMP7 was able to decrease the expression of vimentin in MDA-MB-231 cells thus being positively related to the expression ratio of E-cadherin and vimentin suggesting an important role for

BMP7 in mesenchymal-epithelial transition (Buijs *et al.*, 2007).

Recently, Gao and colleagues have conducted a study focusing on events in the distal metastatic organ and attempting to identify the microenviromental factors that affect metastatic outgrowth. They have identified bone marrow-derived myeloid progenitor cells as responsible for promoting a favourable premetastatic niche. They found an important factor expressed by these cells, the chondroitin sulphate proteoglycan versican, which induced a MET in MDA-MB-231 cells. Interestingly, this factor has also increased the proliferation of MDA-MB-231 cells associated with the acquisition of an epithelial phenotype indicated by an increase in epithelial cell markers and a concomitant inhibition of the mesenchymal marker vimentin (Gao *et al.*, 2012).

Furthermore, previous studies from our laboratory have shown that the over-expression of connexin 43 (Cx43) (the major Cx homolog expressed in normal breast tissue) reduces the invasiveness of MDA-MB-231 cells, as well as their growth rate when cultured on growth factor-reduced EHS (Matrigel) (under 3D culture systems that mimic in vivo conditions) and in immuno-compromised mice, but not in 2D cultures. Moreover, the reduction in growth rate in 3D cultures was accompanied by reduction in the formation of stellate outgrowths characteristic of untransfected cells, and increased formation of spherical clusters that more resemble the growth of normal mammary epithelial cells. Interestingly, Cx43 overexpression resulted in an upregulation of cadherins levels in 2D and 3D cultures and a downregulation in the nuclear levels of β-catenin in 3D cultures of MDA-MB-231 cells. These results point towards a context dependent reduction of tumor phenotype by Cx-43 overexpression in MDA-MB-231 breast cancer cells (Talhouk *et al*., unpublished data).

G. Aim of the study

The general aim of our research project is to confirm the anti-inflammatory effects as well as investigate the potential anti-cancerous activities of the sesquiterpene lactone K100 purified from *cota palaestina subsp. Syriaca.* In order to address the anti-tumor activities of K100 we aimed to perform a comparative study for the effects of K100 *versus* PTL on the tumor phenotype of the highly invasive mammary epithelial cell line MDA-MB-231. Accordingly our specific aims were 1) to show that K100 exhibits PTL-analogous predicted binding to known PTL targets, 2) determine the effect of K100 on key inflammatory mediators, 3) to address the effect of non-cytotoxic concentrations of K100 *versus* PTL on cellular proliferation, cell cycle progression, invasiveness and motility of MDA-MB-231 as well as on the morphology of these cells under 2D and 3D cultures.

CHAPTER II

MATERIALS AND METHODS

A. Cell Culture

MDA-MB-231 human mammary adenocarcinoma cell line was kindly provided by Dr. Mina Bissell (LBNL, CA). MDA-MB-231 cells derived from pleural effusions were grown in humidified incubator (95% air, 5% CO_2) at 37ºC, in RPMI 1640 media (Sigma, Belgium) supplemented with 1% penicillin-streptomycin as well as 10% Fetal Bovine Serum (FBS) (Sigma, St. Louis). This media was changed once every two days. When reaching 80% confluency, cells were washed with 1x Dulbecco's Phosphate Buffered Saline (PBS) then incubated with 2x trypsin (containing 5.0g porcine trypsin, 2.0g EDTA, 4NA per liter of 0.9% NaCl; Sigma, St. Louis) at 37ºC for 1 minute. The cells were washed with 5 ml complete media, and centrifuged at 208x g for 5 minutes, and the pellet was re-suspended in the appropriate amount of media and transferred into new culture plates for maintenance or used for other purposes.

For three-dimensional cultures, we used the Growth Factor Reduced Matrigel obtained from BD Biosciences (BD Biosciences, Discovery Labwork, Two Oak Park, Bedford, MA, BD No. 354230). Thaw Matrigel on ice overnight at 4ºC and store in 1ml aliquots in -80ºC. Matrigel should be handled on ice at all times. Cells were plated in 35 mm tissue culture dishes on top of an EHS reconstituted basement membrane. First, 35 mm culture dishes were placed on ice block in cell culture hood, coated with 500 µl of growth factor-reduced matrigel, then incubated at 37ºC for 30 min to form a bed of 100% solidified EHS measuring approximately 1-2mm in thickness. While the Matrigel is solidifying, count cells and dilute in complete media with 2% EHS, to achieve a final

concentration of 50,000 cells/ml. Clusters start to form by Day 3, and cells were treated with K100and PTL at day 2 and kept in culture for maximum of 5 days.

B. Drug Preparations and Solvent Controls

Drugs used are: parthenolide (BIOMOL-ENZO T-113-0050), prepared in dimethyl sulfoxide (DMSO) and stored at -20ºC, K100, prepared in 98% ethyl alcohol and stored at -20°C. All drugs were stored in the dark for the duration indicated by the manufacturer. Parthenolide stock preparations were aliquoted before freezing and used only once after thawing. In cell culture assays, drug working concentrations contained less than 0.1% DMSO. Control treatments contained up to 0.1% DMSO and 0.5% ethyl alcohol were diluted in culture media.

C. Preparation of Cell Pellet From 3D Cultures

Cells were plated in 35 mm culture plates as described previously, and kept for 3 days in culture. At Day 3, remove old media and wash with 1x Phosphate Buffered Saline (PBS). Place culture dish on ice block and squirt 7 ml 2.5mM PBS-EDTA in each well. Place on ice on rotating shaker for 60 minutes. Collect the volume in each well into 15 ml conicals and leave to settle on ice for 10 minutes. Centrifuge at 200x g for 3 minutes and remove supernatant to dilute EHS. Use cell pellet for cell counting.

D. Protein Extraction and Immunoblotting
1. Total Cellular Protein Extraction

For two-dimensional cultures, MDA-MB-231 cells used for protein extraction are collected at 80% confluency. Cells were scraped into 300 µl of lysis buffer (50mM

Tris-Cl, pH 7.5, 150mM NaCl, 1% Nonidet P40, 0.5% Sodium deoxycholate) to which 40 µl/ml Protease inhibitors (CompleteTM) were added. The mixture was sheared by passage through 27-gauge needle, and then centrifuged at 14,000x g for 30min at 4ºC. The supernatant was stored at -20ºC. DC Protein Assay (Bio-Rad, Hercules, CA) was used to quantify proteins using bovine serum albumin (BSA, Sigma Chemical Co.) as standards. Protein extracts were then mixed with 2x sample buffer with 10% β-mercapto-ethanol in a 1:1 ratio (vol/vol) at the time of gel electrophoresis.

For three-dimensional cultures, total protein extraction is performed by adding 150µl lysis buffer to the cell pellet collected as described previously and pursued similar to extraction from two-dimensional cultures.

2. Extraction of Nuclear Proteins

Cells are gently scraped with 1ml 1x PBS (Lonza, Belgium) into a micro-centrifuge tube and centrifuged at 1000x g for 10 minutes at 4ºC to obtain a cell pellet. The pellet is lysed by rapid freezing and thawing and then resuspended into 70µl of hypotonic Buffer A (10 mM Hepes PH 7.9, 10 mM KCl, 1.5 mM MgCl2, 1 mM Dithiothreitol), incubated for 10 minutes at 4ºC, and then vortexed for 10 seconds. The mixture was centrifuged at 4,500x g for 11 minutes, and the pellet (representing nuclei) was resuspended in 15µl of hypertonic Buffer C (20mM Hepes pH 7.9, 0.4 M NaCl, 1.5 mM MgCl2, 25 % (v/v) Glycerol, 0.2 mM EDTA, 1 mM Dithiothreitol, 0.5 mM PMSF), placed on a shaker for 30 minutes at 4ºC, and then centrifuged at 14,000x g for 20 minutes. The supernatent is diluted with 30 µl of Diluting Buffer D (20 mM Hepes, 50 mM KCl, 20 % (v/v) Glycerol, 0.2 mM EDTA, 1 mM Dithiothreitol, 0.5 mM PMSF) and stored at -20ºC. DC Protein Assay (Bio-Rad, Hercules, CA) was used to quantify

proteins that were then mixed to 2X sample buffer in a 1:1 ratio (vol/vol) at the time of gel electrophoresis.

3. Western Blot Analysis

On basis of equal protein loading, protein extracts were resolved on polyacrylamide gels under denaturing conditions of running buffer (39mM glycine, 48mM Tris base and 0.037% SDS). After electrophoresis, proteins were transferred overnight on immobilin blot PVDF membrane (BioRad, Hercules, CA) using wet blot apparatus in transfer buffer (39mM glycine, 48mM Tris base, 0.037% SDS and 20% methanol). Blocking of the membranes was carried out for 1.5-2 hrs in wash buffer (100mM Tris-Cl, pH 8, 150mM NaCl, 0.1% Tween-20) with 5% skimmed milk, then incubated overnight at 4°C with 1% milk in wash buffer with the primary antibody, of interest (MMP9, P65, Cadherin) (Santa Cruz Biotechnology, Santa Cruz, CA) (dilutions were typically 1:100, 1:1000 and 1:400 respectively). The bound antibody was detected by addition of horse raddish peroxidase-conjugated anti-rabbit IgG or anti-goat IgG (Santa Cruz Biotechnology, Santa Cruz, CA) followed by enhanced chemiluminescence (ECL, Santa Cruz). All incubations were performed at room temperature. Equal loading was determined by probing total extracts for mouse anti-GAPDH (1:10000-v/v) and probing nuclear extracts for Lamin A/C (1:1000-v/v).

E. Cell Counting by Trypan Blue

MDA-MB-231 cells were plated in 24-well tissue-culture plates at a density of 3.5×10^4 cells in each well. The cells were counted from triplicates after 24, 48, 72, and 96 hrs. First, media was removed, and the cells subsequently trypsinized and collected

in the initial media of each plate that contains dead cells. Cells were then diluted in Trypan Blue (1:1) ratio (vol/vol) and counted using a hematocytometer. Experiments were repeated at least three times.

For three-dimensional cultures, MDA-MB-231 cells were plated in triplicates in 24-well tissue-culture plates at a density of 2×10^4 cells in each well. The cells were maintained for 3 days before counting. At day 2 cells were treated with K100 and PTL and at day 3, cell pellet was collected as described previously and trypan blue counting was pursued similar to counting from two-dimensional cultures.

F. Three-Dimensional Morphogenesis Assay

MDA-MB-231 cells were plated in 35 mm culture dishes as described previously. Ten fields of each well were imaged at low power. Colony morphology was quantified by counting the number of spherical *versus* stellate colonies within each image. Equal numbers of colonies were counted, and % stellate colonies of total were calculated. A colony was considered stellate if it had two or more extensions from the central colony of cells.

G. Invasion Assay

Six-well tissue-culture plates were fitted with inserts (8 μm pore size) that have been coated with growth factor-reduced EHS (Matrigel). Endothelial cells (ECV304) were grown in the inserts to confluency, and then seeded with MDA-MB-231/GFP tumor cells pretreated for 24 hrs with K100 and PTL. After 16 hrs of co-culture, inserts were removed and the endothelial cell layer was gently removed using a cotton swab. The membrane of the insert was then removed and mounted on a microscopic slide and

examined by fluorescence microscopy. Fluorescent tumor cells that successfully

invaded through the endothelial layer were counted, and are plotted on a histogram as

percentage of invaded control cells.

H. Motility Assay

Six-well tissue-culture plates were fitted with inserts (8 μm pore size). The inserts were

coated with 300μl of EHS-Growth media solution of 1:5 ratio and incubated at 37°C for

4 hrs. 1.3×10^5 MDA-MB-231 cells were seeded in the inserts. After 24 hrs, the cells

were treated for 16 hrs with K100 and PTLand then fixed using 4% 53 formaldehyde in

PBS for 20 minutes at room temperature (or kept at 4ºC for a maximum of 2 weeks).

The cells towards the inside of the insert were removed by using a cottonswab, and

nuclie of migrated cells were counterstained with Hoechst (DAPI; 4,6-diamino-2-

phenylindole) (Molecular Probes, Eugene, OR, USA) at a concentration of 0.5 μg/ml,

for 10 minutes at RT. The insert is then cut and mounted on a microscopic slide using

Vector labs hardmount fluorescence media. The inserts were then examined by

fluorescence microscopy. Cells that successfully moved through the 8μm pores were

counted (10 random fields at X magnification), and were then plotted on a histogram as

percentage of motile cells relative to the control cells.

I. Cell Cycle Analysis

Cells were trypsinized at 70% confluency for 2D cultures, and at Day 8 for 3D cultures,

were collected by centrifugation a 208x g for 5 min at 4ºC and were fixed in ice-cold

70% ethanol for a minimum of 2 hrs and a maximum of 2 weeks. Cells were then

centrifuged (208x g, 5 min, 4ºC) and the pellet was washed with 1X PBS. DNase free

RNase A was added at a concentration of 0.2mg/ml (50 µl) and cells were kept at 37 ºC

in a water bath for 1 hr and 30 minutes to allow full digestion of RNA. The pellet was

washed twice in 1X PBS before final re-suspension in 420 µl of 1X PBS into flow tubes

(BD falcon, USA). 30 µl of 2 mg/ml propidium iodide were then added to each flow

tube and the cells were then analyzed using the flow cytometer.

J. SDS-Substrate Gel Electrophoresis (Zymography)

Gelatinase activity in the medium samples was analyzed. Equale sample volumes were

loaded on 30% and run on 10 % polyacrylamide gel imprenated with gelatin(100X).The

gels were run in electrophoresis running buffer (25 mM TRIS-base, 192mM glycine; 0.1

% SDS, water). After that, the gels were washed twice for 30 min in 2.5% Triton X-100

solution. After washing the gels were incubated for 16-20 hrs in development buffer

(50mM Tris HCl; 5mMCaCl2; 0.02%NaN3; 0.5 %Triton X; Water). The gels were then

stained for at least 2 hours, at room temperature, in 0.1 % comassie blue R-250, in 50%

methanol, and 10% acetic acid. The gels were then destained for 15 min in destaining

solution (MeOH: acetic acid: water 4.5:1:4.5). The gelatinases activity was visualized as

clear white bands on darkly stained blue gels and analyzed by Gel documentation (Bio

RAD) using the software Quantity 1.

K. Griess reaction assay of NO.

The analysis of NO was accomplished by the Griess assay for nitrite (the spontaneous

oxidation product of NO) using a Griess Reagent Kit (Invitrogen) involving addition of

20 µl of Griess Reagent (0.05% N-(1-napthyl) ethylenediamine dihydrochloride, 0.5%

sulfanilic acid in 2.5% phosphoric acid) to 150 µl of nitrite-containing sample or

standard and 130 µl deionized water, per the manufacturer's instructions. The color

developed by azo dye formation in proportion to nitrite concentration (µM) in solution

was quantified using a spectrophotometer (thermo labsystems multiskan EX) at

wavelength 540 nm. Samples were assayed in duplicates and data is represented as the

average concentration of NO2- (µM) of duplicate samples ± SD (standard deviation).

L. Immunoassay of Interleukin-6.

To measure IL-6 secretion in response to ET in SCp2 cells, medium collected 24 hrs

post-ET treatment and was assayed by enzyme linked immunosorbent assay (ELISA)

for IL-6 (Max Deluxe set mouse IL-6 , Biolegend) according to the manufacturer's

protocol. The IL-6 ELISA was performed in 96 well plates, capture mouse IL-6

antibody were coated overnight at 4 C, blocking was done using assay diluents provided

by the kit, then samples were diluted 4 times and added to the wells after 2 hours the

secondary (detection) antibody was added for one hour followed by the addition of

horseradish-peroxidase Avidin (HRP). This was followed by the addition of HRP

substrate TMB that yielded color intensity in proportion to the amount of IL-6 present in

the sample. Samples were analyzed using spectrophotometer (thermo labsystems

multiskan EX) at a wavelength of 450 nm. Samples assayed in duplicate and data is

represented as the average pg IL-6 / ml of duplicate samples ±SD.

M. Molecular Docking

The possibility of binding,precise location of binding sites and mode of binding foreach

ligand was carried out independently using an automateddocking software, Molgro

Virtual Docker 2010, version 4.2(Molgro ApS, Aarhus, Denmark, http://molegro.com),

that isbased on guided differential evolution and a force field basedscreening function (Friesner *et al.,* 2004; Thomson and Christensen, 2006). The entire protein structures were obtained from the Protein Data Bankand were loadedon to MVD platform for docking process. MVD performsflexible ligand docking, so the optimal geometry of theligand is determined during the docking. MVD includesMolDock Score and PLANTS Score for evaluatingdocking solutions. MVD returns multiple posesrepresenting different potential binding modes. Multiple runs were done for each ligand and the results shown represent the average of five independent simulations.

N. Statistical Analysis

Data presented are the means ± SD of at least two independent experiments or as indicated. Significant differences were determined using the post -hoc tests; Tukey, SNK and Dunnett tests of the SPSS Version 16.0 software. Significance was set at indicated p-values (0.05, 0.01 or 0.001).

CHAPTER III

RESULTS

A. *In Silico* Molecular Docking Shows that K100 Exhibits PTL-Analogous Predicted Binding to Known PTL Targets

K100, as referred to in our studies is the bioactive molecule extracted from

Cota palaestina subsp. syriaca.K100 bears similar functional goups to those found in

PTL, namely an exocyclic α-methylene-γ-lactone ring and an epoxide moiety(Talhouk

and Saliba*et al*., unpublished data). Given this structural homology between K100 and

PTL and knowing that the biological activities of PTL including its anti-cancer and anti-

inflammatory properties are primarily attributed to binding and inhibiting the function

of the NF-kB, JAK-STAT and TNFα signaling pathways (Pajak *et al*., 2008), and

knowing that the more soluble and orally bioavailable PTL analogue, dimethylamino-

PTL (DMAPT), which has similar effects to those of PTL *in vitro* as well as *in vivo* is

currently under clinical trials (Guzman *et al*., 2009), we sought to assess the ability of

K100 to bind *in silico* to different PTL targets. Accordingly, we initiated our study by

performing a bioinformatics docking analysis *in silico*, which predicts the site and

affinity of binding of four possible K100 isomers to known protein targets of PTL

which are key factors of the above mentioned signaling pathways including IKKB, p65,

JNK1, JNK2, Stat3b, Stat6, TNFR1, and GSH. Although this study is predictive, and

provides rough estimates of binding affinities, it provides an initial platform regarding

the similarity in terms of physiological effects between the two molecules. In order to

enhance the analytical efficacy of the docking analysis, we included in the docking's

simulation two other SLs variants bringing the total number of molecules to seven: the

more soluble and bioavailable PTL analogue DMAPT and Salograviolide A (SAL

A)(Figure 12A), another SL previously identified by our laboratory and derived from *Centaurea ainetensis* (Talhouk *et al*. 2008). Molecular docking simulations of the aforementioned SLs to IKKB, predicted that all seven molecules bind to this protein at the same cleft (Figure 12B). However, each of these molecules is predicted to bind to IKKb with a different affinity which is measured in Kcal/mol where smaller values indicate larger affinities. Interestingly, the affinity of binding of the four K100 isomers (-19.2, -19.5, -18.6 and -18 kcal/mol) was estimated to be very similar to that of PTL (-19.7 kcal/mol), unlike the two other variants DMAPT (-14.2 kcal/mol) and SAL A (-17.8 kcal/mol) (Figure 12C). Similarly, when we performed docking simulations against other protein targets, the affinity of binding of the four K100 isomers to the PTL targets was either equal to that of PTL, or second best to it. Moreover, statistical analysis indicates that the avergage binding affinity of the four K100 isomers to protein targets of PTL is similar to that of PTL and statistically higher than that of DMAPT. However, it is similar to that of SAL A in some proteins and different in othersindicating that K100 can specifically bind to all tested targets with comparable binding affinities to PTL.

A-

K100 - 1 K100 - 2 K100 - 3 K100 - 4

Parthenolide (PTL) Dimethylamino Parthenolide (DMAPT) Salograviolide A (Sal A)
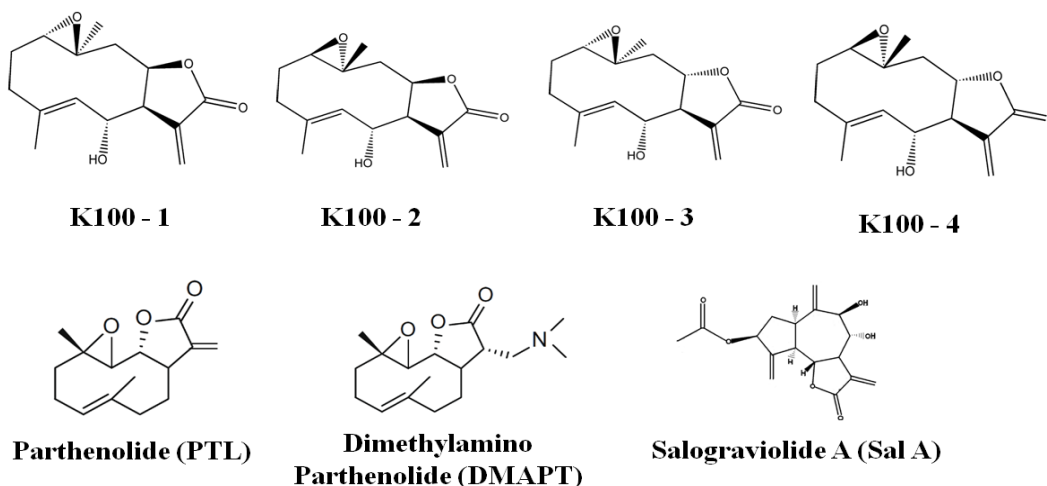
B-
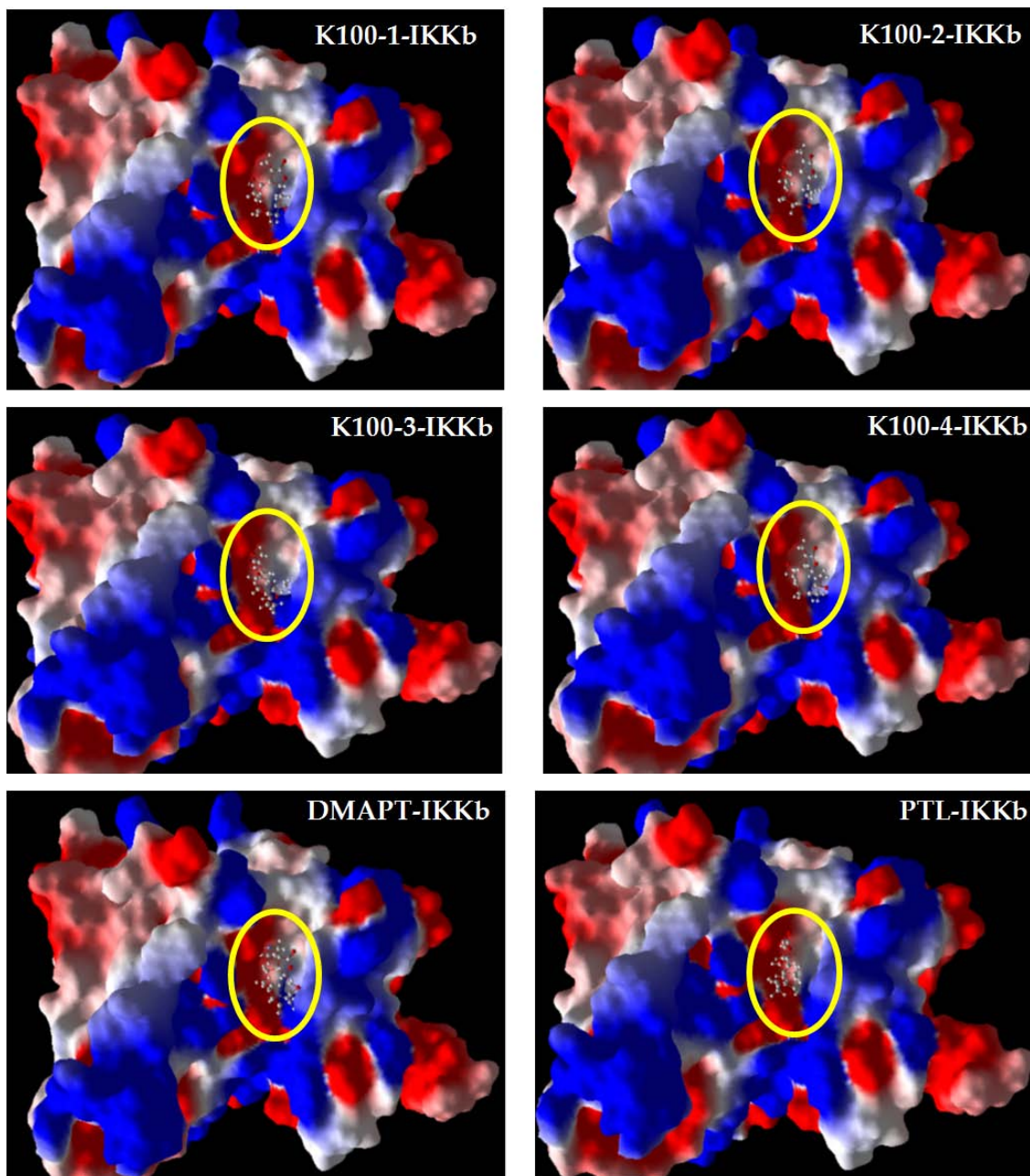
C-

Protein	Ligand	Affinity (Kcal/mol)	SD	Significance
Actin	DMAPT	-17.6	0.0	* * *
	k100(1)	-21.4	0.0	
	K100(2)	-19.6	0.0	
	K100(3)	-21.0	0.0	
	K100(4)	-18.8	0.0	
	Parthenolide	-22.2	0.9	* * *
	Salograviolide A	-18.5	0.1	* * *
GAPDH	DMAPT	-15.7	0.1	
	k100(1)	-19.9	0.5	
	K100(2)	-20.8	0.0	
	K100(3)	-20.2	0.0	
	K100(4)	-19.4	0.0	
	Parthenolide	-21.8	0.0	
	Salograviolide A	-19.4	0.4	
Albumin	DMAPT	-14.5	0.2	* * *
	k100(1)	-19.7	0.0	
	K100(2)	-19.4	0.1	
	K100(3)	-18.6	1.0	
	K100(4)	-19.3	0.0	
	Parthenolide	-19.5	0.0	
	Salograviolide A	-17.9	0.9	

Protein	Ligand	Affinity (Kcal/mol)	SD	Significance
P38	DMAPT	-14.4	0.5	* * *
	k100(1)	-18.4	0.3	
	K100(2)	-19.4	0.2	
	K100(3)	-20.2	0.2	
	K100(4)	-19.4	0.5	
	Parthenolide	-19.8	0.8	
	Salograviolide A	-18.6	0.4	
Stat3b	DMAPT	-14.6	0.9	* * *
	k100(1)	-19.3	0.8	
	K100(2)	-18.7	0.5	
	K100(3)	-18.0	0.4	
	K100(4)	-18.7	0.5	
	Parthenolide	-20.1	0.4	
	Salograviolide A	-17.4	0.7	
Stat6	DMAPT	-15.1	0.2	* * *
	k100(1)	-19.4	0.1	
	K100(2)	-19.1	0.6	
	K100(3)	-18.3	0.8	
	K100(4)	-18.4	0.4	
	Parthenolide	-20.4	0.8	
	Salograviolide A	-17.4	1.1	

Protein	Ligand	Affinity (Kcal/mol)	SD	Significance
GSH	DMAPT	-16.4	1.1	* * *
	k100(1)	-21.1	0.0	
	K100(2)	-18.7	0.6	
	K100(3)	-17.6	0.0	
	K100(4)	-20.9	0.0	
	Parthenolide	-21.6	0.6	
	Salograviolide A	-19.3	1.0	
TNFR1	DMAPT	-14.3	0.2	* * *
	k100(1)	-19.2	0.4	
	K100(2)	-18.8	0.2	
	K100(3)	-18.8	0.0	
	K100(4)	-18.9	0.0	
	Parthenolide	-19.9	0.0	
	Salograviolide A	-16.5	0.6	* * *
IKKb	DMAPT	-14.2	0.3	* * *
	k100(1)	-19.2	0.5	
	K100(2)	-19.5	0.0	
	K100(3)	-18.6	0.3	
	K100(4)	-18.0	0.9	
	Parthenolide	-19.7	0.2	
	Salograviolide A	-17.8	0.5	

Protein	Ligand	Affinity (Kcal/mol)	SD	Significance
P65	DMAPT	-15.1	0.3	* * *
	k100(1)	-18.9	0.0	
	K100(2)	-19.5	0.3	
	K100(3)	-18.2	0.4	
	K100(4)	-19.1	0.1	
	Parthenolide	-20.3	0.3	
	Salograviolide A	-17.4	1.1	
JNK1	DMAPT	-15.5	0.9	* * *
	k100(1)	-19.7	0.5	
	K100(2)	-21.2	0.0	
	K100(3)	-17.6	0.0	
	K100(4)	-19.0	0.0	
	Parthenolide	-21.6	0.0	
	Salograviolide A	-20.1	1.1	
JNK2	DMAPT	-16.3	0.7	* * *
	k100(1)	-19.2	0.5	
	K100(2)	-17.6	0.3	
	K100(3)	-18.8	0.2	
	K100(4)	-18.5	0.6	
	Parthenolide	-19.5	0.0	
	Salograviolide A	-16.8	0.1	* * *

Figure 12. Bioinformatics docking analysis of seven SLs to known targets of PTL.**(A)** Chemical structure of the four K100 isomers and the other three SLs included in the docking simulations: PTL, DMAPT and SAL A. **(B)** Electrostatic surface of the IKKb protein with predicted binding positions of K100 (1), K100 (2), K100 (3), K100 (4), PTL, DMAPT and SAL A in a general overview. Yellow circles enclose the docked SLs. **(C)** Predicted binding affinities of K100 (1), K100 (2), K100 (3), K100 (4), PTL, DMAPT and SAL A to IKKb, p65, p38, JNK1, JNK2, Stat3b, Stat6, TNFR1, GSH, Actin, GAPDH and Albumin. Numbers shown represent averages of 5 independent simulations ± standard deviation (SD). Statistical significance is represented by asterisk (***) at $p < 0.001$.

B. K100 Inhibits Endotoxin-Induced Pro-Inflammatory Markers: IL-6, MMP9 and NO in SCp2 Cells

Previous studies from our laboratory have shown that the water extract of Cota palaestina exhibits anti-inflammatory activities (Talhouk *et al*., 2007); however the active molecules mediating these affects were not identified. Therefore, after identifying the structure of the active molecule *in vitro* (Fares MB. Thesis Appendix, 2010), K100, that is mediating these anti-inflammatory activities, and noting that inflammation is a critical component of tumor progression, we sought to check the effect of K100 on other inflammatory mediators common between cancer and inflammation mainly MMP9, NO and IL6 in endotoxin (ET)-stimulated SCp2 normal mammary epithelial cells. As such, K100 anti-inflammatory activities were evaluated employing an *in vitro* model of ET-induced inflammation in normal mouse mammary epithelial SCp2 cells. The effect of K100 on levels of IL-6, NO and MMP9 produced by SCp2 cells as a result of ET stimulation was analyzed after treating cells with non-cytotoxic concentrations of K100 (5, 10, 15, 20 µM). Cells were treated with the plant extracts 30 min prior to ET stimulation and 24 hrs later media was collected and analyzed for their production of NO (Griess reaction assay), MMP-9 (Zymography), and IL-6 secretion (ELISA immunoassay). Interestingly, in line with previous results from our laboratory (Fares MB. Thesis Appendix, 2010), K100 caused a dose-dependent downregulation of ET-

induced IL-6 levels with an inhibition reaching 83 % at 20 µM concentration (Figure 13A).

SCp2 cells in culture produce abundant levels of gelatinase A in ET-treated and untreated cells; however gelatinase B is markedly upregulated in ET-treated cells. K100 inhibited, in a dose dependent manner, MMP-9 (Gelatinase B) in a conditioned media at 24hrs post ET-treatment reaching a 40% decrease at 20 µM. However, only partial inhibition of MMP-2 (Gelatinase A) was observed with 15 and 20 µM concentrations at 24hrs post ET-treatment (Figure 13B). Furthermore, K100 was able to inhibit NO production in ET inducedSCp2 cells in a dose dependent manner with significant inhibition reaching 56% at a concentration as low as 5 µM. In the three experiments K100 did not cause a significant change in the levels of IL-6, NO and MMP9 in control SCp2 cells not treated with ET (Figure13C).

A-
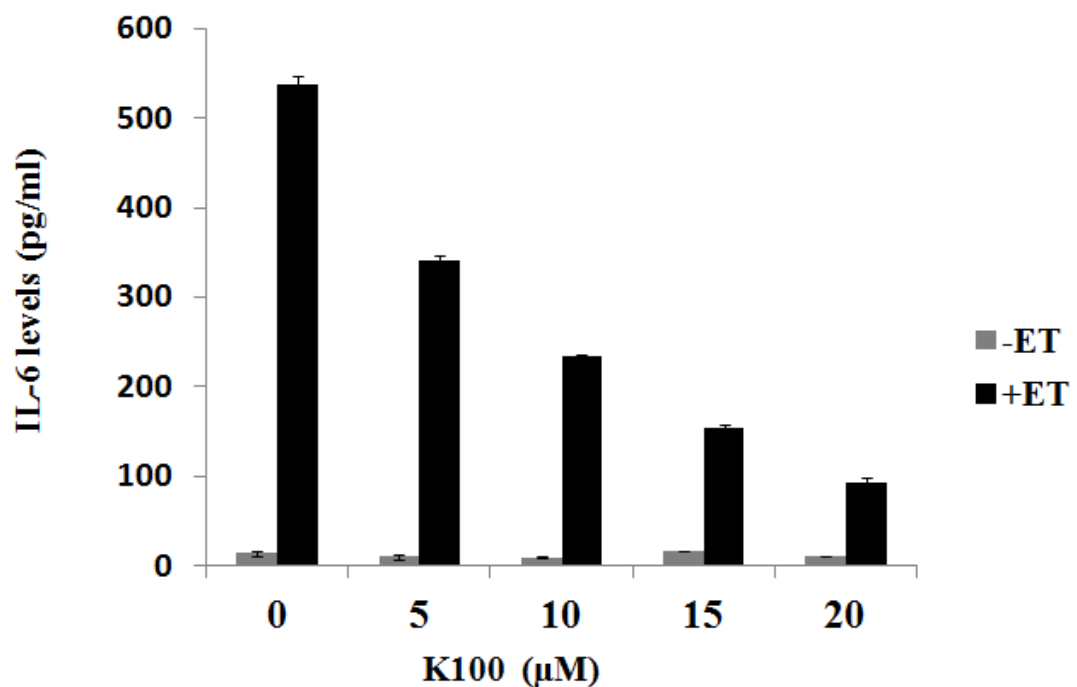
B-
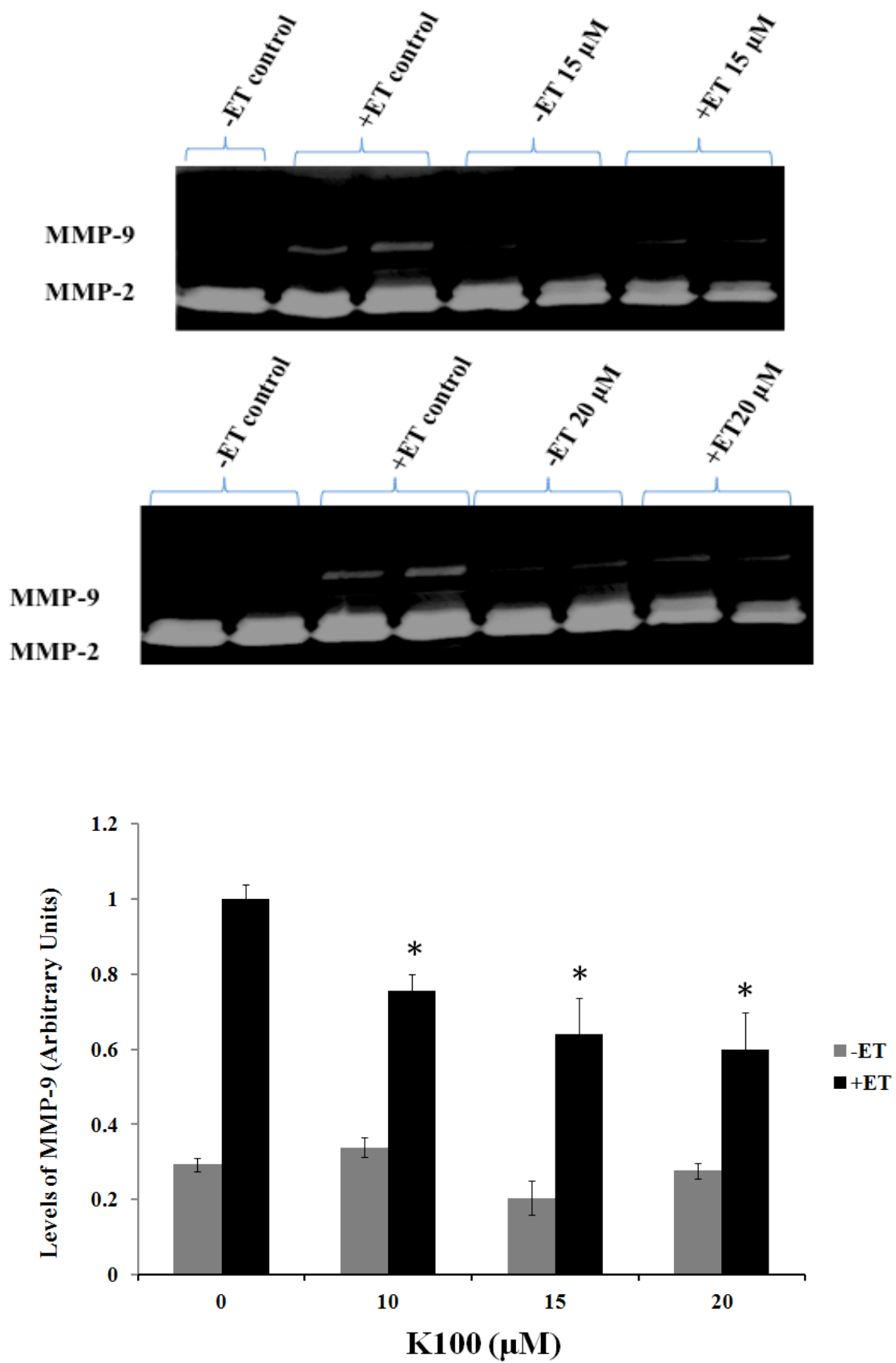
C-
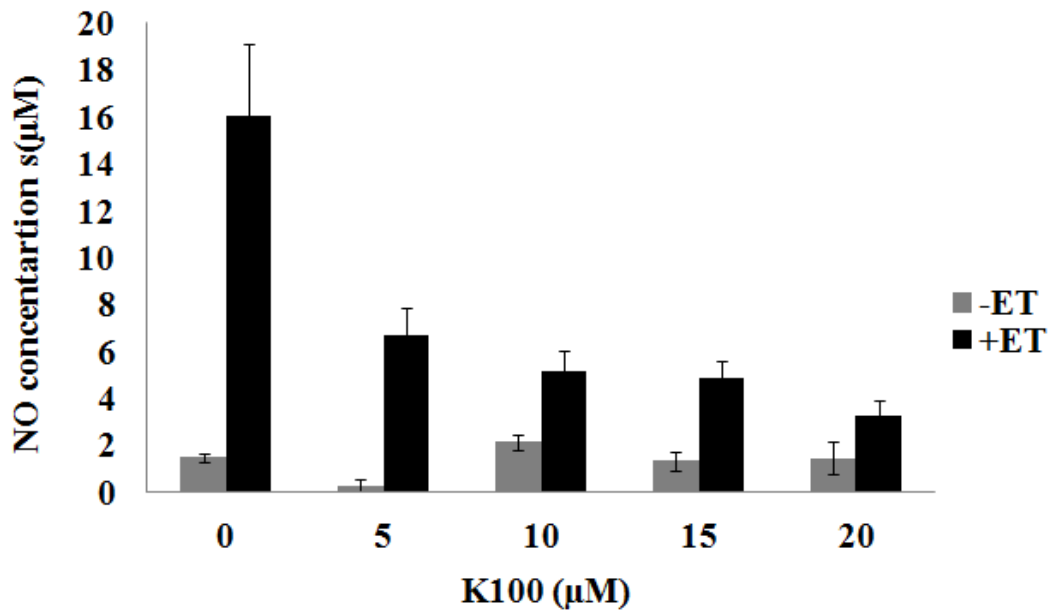

Figure 13. Effect of different concentrations of K100 on levels of ET-induced IL-6, NO and MMP9 in SCp2 cells. Cells were treated with 0, 5, 10, 15 and 20 µM of K100 and media samples were collected 24 hrs post ET-stimulation and analyzed for their NO production (Griess reaction assay) (**A**), MMP-9 and MMP-2 production (Zymography) (**B**), and IL-6 secretion(ELISA immunoassay) (**C**). Reults represent the averages ± SD of two independent experiments. Statistical significance is represented by asterisk (*)at $p<0.05$.

C. MDA-MB-231 Cells Exhibit Different Morphology in 2D and 3D Cultures

MDA-MB-231 cells are human mammary adenocarcinoma cells derived from pleural effusions. These cells were derived from a metastatic adenocarcinoma of the mammary gland of a 51-year-old Caucasian woman, according to the data sheet of the American Type Culture Collection (ATCC). MDA-MB-231 cells, with epithelial-like morphology, appear phenotypically as spindle shaped cells. They adhere and grow as monolayers on plastic cultures as shown in (Figure 14A). On the other hand, MDA-MB-231 cells form 3D stellate colonies when cultured on growth factor-reduced EHS (Matrigel) as shown in Figure 14B.
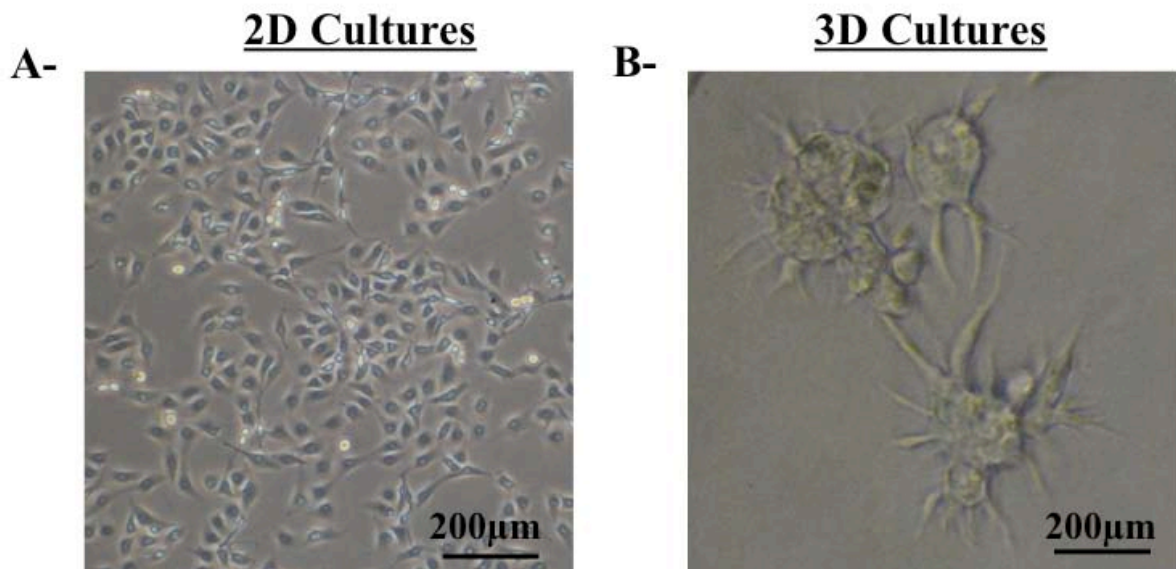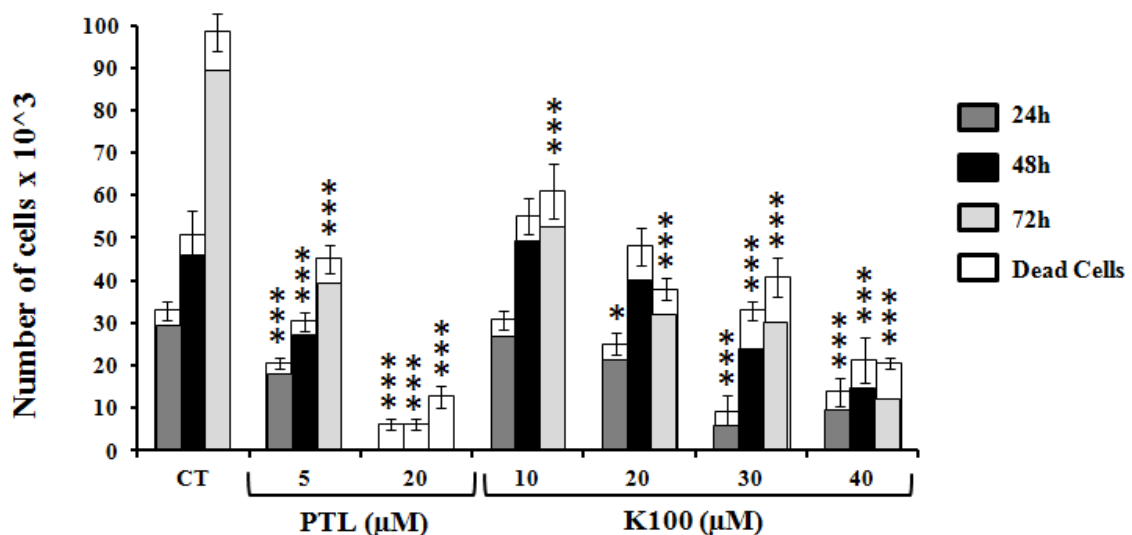
Figure 14. Morphology of MDA-MB-231 cells in 2D and 3D culture conditions. (A) Phase contrast photomicrographs of MDA-MB-231 cells cultured on plastic. (B) Phase contrast photomicrographs of MDA-MB-231 cells cultured on growth factor reduced matrigel.

D. K100 and PTL Decrease the Proliferation Rate and Does Not Affect the Morphology of MDA-MB-231 Cells in 2D Cultures

Given that PTL has been shown to suppress the proliferation and to induce apoptosis in many human cancer cells *in vitro*, such as hepatoma, human lung carcinoma (A549) and human medulloblastoma (TE671) (Parada *et al.,* 2007), and knowing that K100 exhibited PTL-analogous predicted binding to several PTL targets, we sought to establish whether K100 actually exhibits PTL analogous effects, particularly anti-proliferative ones in cancer cells. Therefore, we assessed the effect of K100 as well as PTL on MDA-MB-231 cell growth and proliferation on plastic. Cells were treated with different concentrations of K100 and PTL and the number of living and dead cells was counted using the trypan blue dye exclusion assay at 24 hrs time-intervals after plating. In line with our previous results (Fares MB. Thesis Appendix, 2010), K100, at noncytotoxic concentrations of 10 and 20µM inhibited the growth of MDA-MB-231 cells in a dose-dependent manner. PTL also inhibited the growth of

MDA-MB-231 cells at 5µM concentrations and showed high toxicity at 20 µM concentrations (Figure 15A). Moreover, previous studies from our laboratory have determined the cytotoxicity profile of K100 *versus* PTL on normal (MCF-10A) and cancerous (MCF-7 and MDA-MB-231) mammary epithelial cells showing that both K100 and PTL inhibited the growth of the two cancerous cell lines in a dose dependent manner, and at concentrations tolerable by normal cells (Fares MB. Thesis Appendix, 2010). In light of all these results, we chose 10µM K100 and 5µM PTL as the effective non-cytotoxic working concentrations in breast cancer cells. Furthermore, photomicrographs for untreated MDA-MB-231 cells *versus* MDA-MB-231 cells treated with these non-cytotoxic concentrations of K100 *versus* PTL (10µM K100, 5µM PTL) for 24hrs show that these cells grow similarly towards forming monolayers when cultured on plastic and with similar morphologies (Figure 15B).
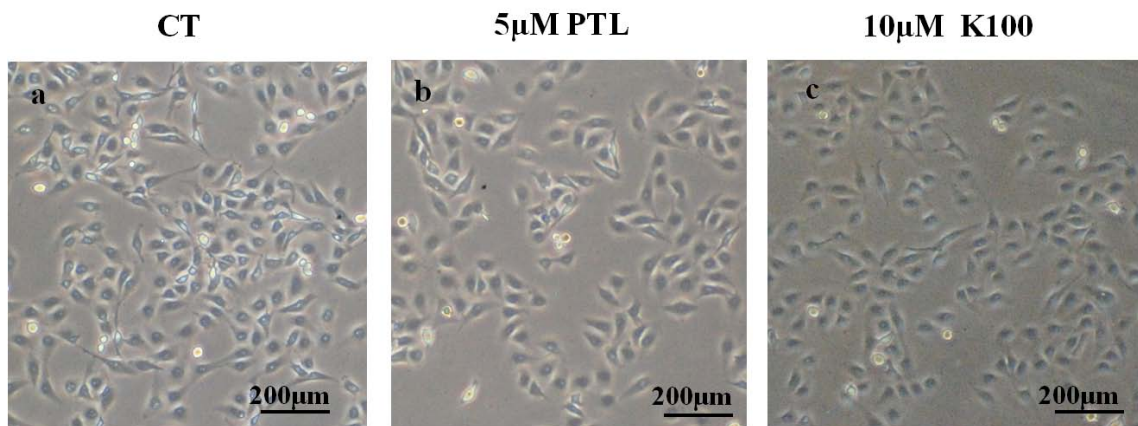
A-

B-

Figure 15. Effect of K100 *versus* PTL on the proliferation and morphology of MDA-MB-231 cells. (**A**) Effect of different concentrations of K100 *versus* PTL on MDA-MB-231 cells after treatment for 24, 48 and 72 hrs on cellular viability as measured by trypan blue exclusion dye assay. (**B**) Phase contrast photomicrographs of untreated MDA-MB-231 cells (**a**) and those treated with 5µM PTL (**b**) and 10µM K100 (**c**) 24 hrs post treatment.Reults represent the averages ± SD of two independent experiments. Statistical significance comparing number of number of cells at each time point to its control is represented by (***) asterisk indicating significant difference at p<0.001, (**) asterisk indicating significant difference at p<0.01 and (*) asterisk indicating significant difference at p<0.05.

E. K100 and PTL Prolong the S Phase of the Cell Cycle of MDA-MB-231 Cells in 2D Cultures

10 µM K100 and 5µM PTL decreased the proliferation rate of MDA-MB-231. As such, we sought to assess the effect of 10µM K100, 5µM PTL on cell cycle progression of MDA-MB-231 cells grown under 2D culture conditions at 80% confluency using propidium iodide (PI) cell cycle analysis. This decrease in cell proliferation was accompanied by a 86% prolongation of S-phase of the cell cycle in cells treated with 10µM K100 compared to a 71% prolongation in cells treated with 5µM PTL. On the other hand, no significant differences were noted in pre G0/G1, G0/G1 and G2/M phases of the cell cycle when comparing cells treated with K100 *versus* PTL with untreated cells (Figure 16A,B).

A-

	CT	PTL(5µM)	K100(10µM)
Pre G0/G1	4 ± 1	5 ± 2	3 ± 1
G0/G1	68 ± 6	56 ± 7	59 ± 3
S	7 ± 1	12 ± 1	13 ± 1
G2/M	21 ± 6	27 ± 5	25 ± 3

B-
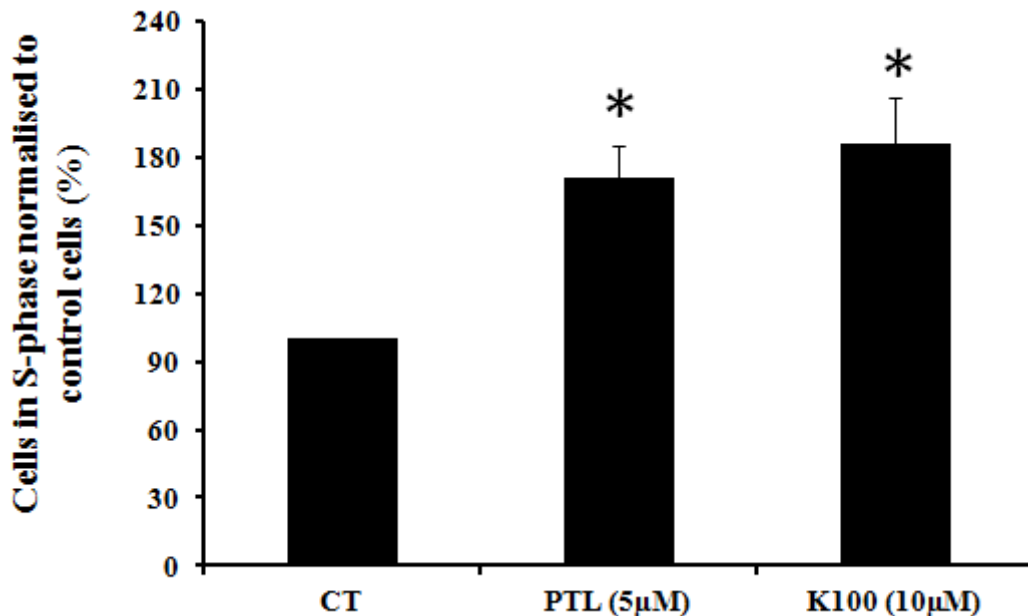
Figure 16. Effect of K100 *versus* PTL on cell-cycle progression of MDA-MB-231cells under 2D culture conditions.(A) Table representing percentage of cells in G0/G1, S and G2/M phases of cell cycle in control cells and cells treated with K100 *versus* PTL. (B) Histogram plot showing cell counts in S phase with respect to untreated cells.Reults represent the averages ± SD of two independent experiments. Statistical significance is represented by (***) asterisk indicating significant difference at p<0.001, (**) asterisk indicating significant difference at p<0.01 and (*) asterisk indicating significant difference at p<0.05.

F. K100 and PTL decrease the Proliferation Rate of MDA-MB-231 Cells in 3D Cultures

3D *in vitro* models are thought to span the gap between 2D and *in vivo* animal models. Adding more to the importance of 3D culture systems, it is now known that signaling pathways that are crucial in cancer progression behave differently in 3D and 2D cultures. For these reasons, drug testing must be done also in 3D culture (Bissell *et al*. 2002). Therefore, we assessed the effect of K100 and PTL on growth and proliferation of MDA-MB-231 cells cultured on growth factor reduced matrigel. Similar to 2D cultures, treatment of MDA-MB-231 cells with different concentrations of K100 *versus* PTL significantly decreased the growth rate of MDA-MB-231 cells. In fact, when cell number was monitored after 3 days of culture and 24 hrs post treatment using the trypan blue dye exclusion assay, the number of cells treated with K100 was reduced in a dose-dependent manner starting with approximately 30% reduction at 10μM reaching more than 50% at 40μM with a cell death percentage not exceeding 14% in treted cells. Similarly, the growth of cells treated with PTL was reduced by approximately 30% but with a higher % of dead cells which was around 20% (Figure 17).
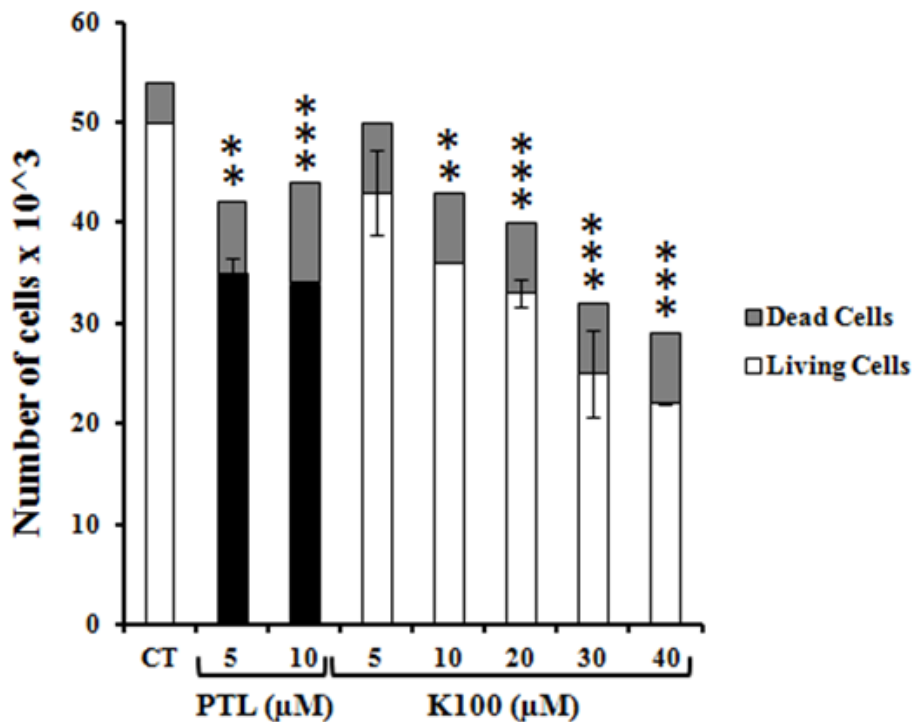
Figure 17. Effect of K100 *versus* PTL on the proliferation rate of MDA-MB-231 cells in 3D culture conditions over three days. Bargraph showing number of untreated, K100-treated, and PTL-treated MDA-MB-231 cells at day 3 of culture. Reults represent the averages ± SD of two independent experiments. Statistical significance is represented (*)asterisk indicating significant difference at $p < 0.05$.

G. K100 and PTL Induce Spherical Cluster Formation and Decreases the Size of Spherical Colonies of MDA-MB-231 Cells in 3D Cultures

MDA-MB-231 cells form disorganized structures (stellate colonies) when cultured on growth factor reduced matrigel, which is typical of malignant cells. In order to assess whether K100 *versus* PTL affect the morphology of MDA-MB-231 cells under 3D culture conditions, MDA-MB-231 cells cultured on matrigel were treated with different concentrations of K100 as well as PTL and photomicrographs were taken at day three of culture. Interestingly, cells treated with K100 as well as PTL exhibited different morphologies than that of untreated cells after three days in culture. In fact, most of the untreated cells form stellate colonies upon adhering to the growth factor

52

reduced matrigel, which is typical of malignant cells; however cells treated with K100 and PTL showed an increase in the percentage of spherical colonies that resemble the growth of normal mammary epithelial cells on growth factor reduced matrigel (Figure 17 A,B). By counting stellate and spherical colonies that formed at day 3 in 3D cultures of untreated, K100-treated and PTL- treated cells, it was clear that treatment with K100 increased the percentage of spherical colonies as compared to untreated cells in a dose-dependent manner starting with approximately 35% at 10 µM up to 65% at 40 µM in which 97% of the cells are spherical. Similarly, treatment with PTL caused an increase in the percentage of spherical colonies as compared to untreated cells with approximately 25% at 5µM up to 40% at 20 µM (Figure 17B).

Photomicrographs of cells grown in 3D cultures reflected the previously noted decrease in proliferation upon treatment with K100 *versus* PTL and showed a significant difference in colony sizes in cells treated with K100 *versus* PTL compared to untreated cells. In fact, cluster size grouping, based on cluster diameter, showed that small sized clusters (diameter between 10-35 μm) were abundant in cells treated with K100 reaching 77% of total clusters upon treatment with 40μM K100 compared to 7% in untreated cells. Moreover, the percentage of large sized clusters (diameter larger than 100 μm) decreased dose-dependently in cells treated with K100 reaching 6% with 40μM K100 compared to 74% in untreated cells (Figure 17C). On the other hand, cells treated with 5μM PTL had the same percentage of small sized clusters (9%) as that of untreated cells (8%), but these cells showed an increase in percentage of medium sized clusters (diameter between 70-100 μm) and a decrease in large sized clusters as compared to untreated cells.
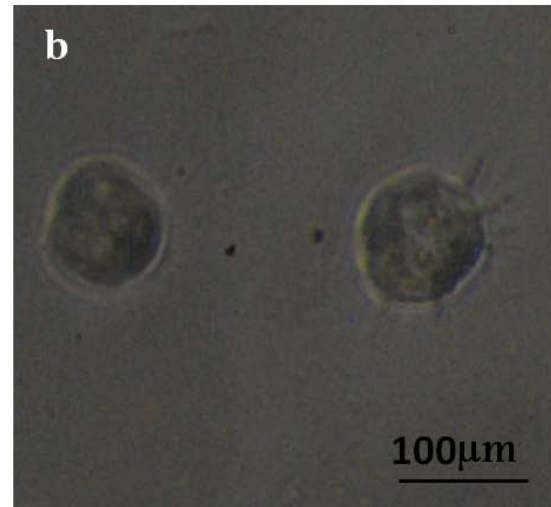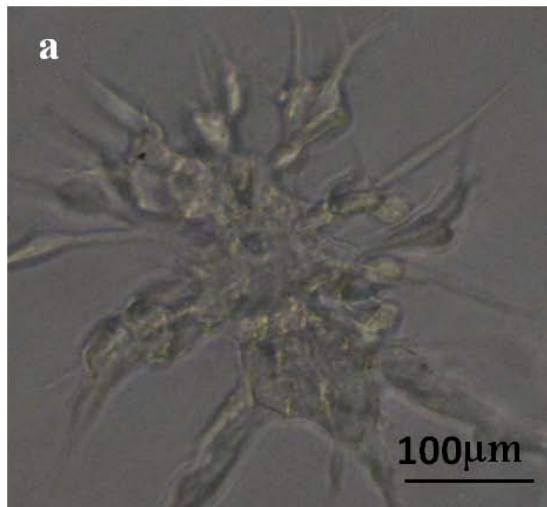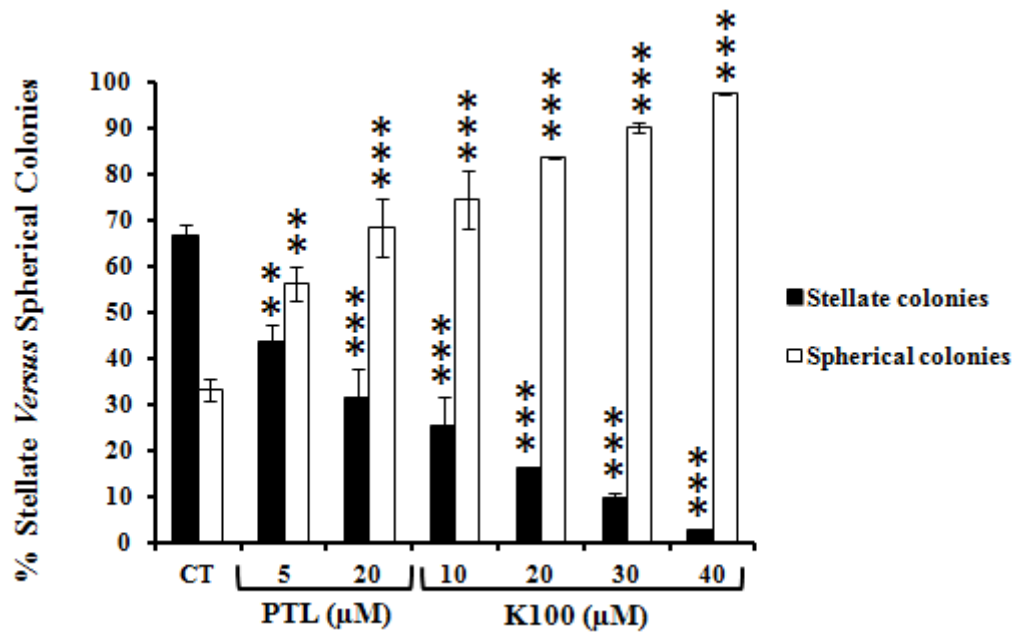
A-

Stellate Colony **Spherical Colonies**

B-

B-
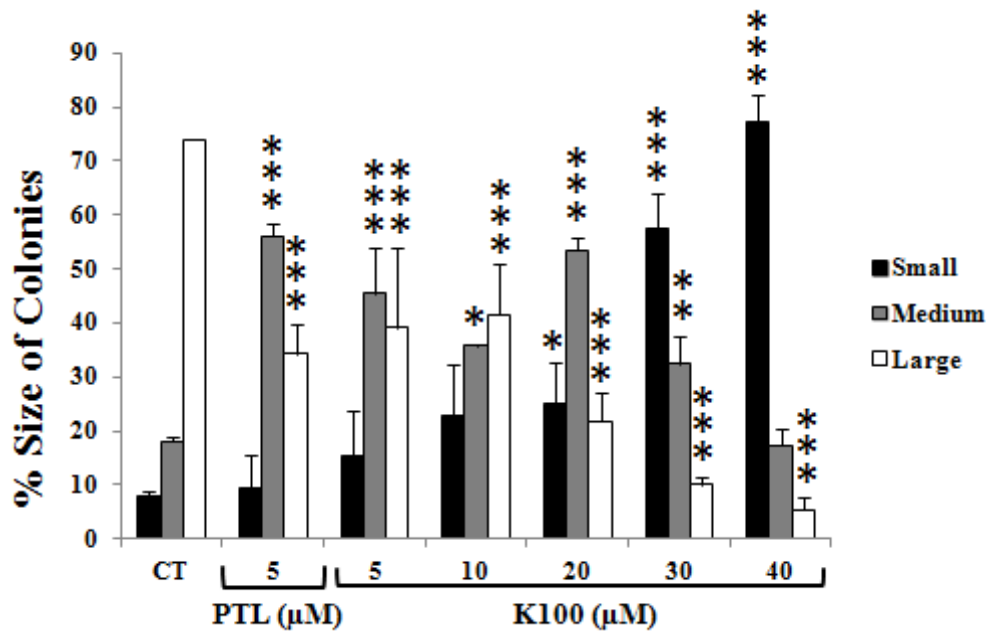
Figure 18. Effect of K100 *versus*PTL on the morphology of MDA-MB-231 cells in 3D culture conditions over three days. (**A**)Phase contrast photomicrographs of MDA-MB-231 cells (a,b) *versus* fluorescent pictures of MDA-MB-231/GFP (c,d) showing stellate colonies (a,c) of untreated cells and spherical colonies (b,d) obtained upon treatment with K100 *versus* PTL. (B) Histogram showing percent stellate *versus* spherical colonies of untreated and K100 *versus* PTL treated MDA-MB-231 cells at day 3. (C) Histogram showing colony sizes analysis, after grouping colonies in 3D cultures into small (less than 70 µm), medium (between 70 and 100 µm) and large (greater than 100 µm). Reults represent the averages ± SD of three independent experiments. Statistical significance comparing % size of colonies of each size group to its control is represented by (***) asterisk indicating significant difference at $p<0.001$, (**) asterisk indicating significant difference at $p<0.01$ and (*) asterisk indicating significant difference at $p<0.05$.

H. K100 and PTL Decrease the Trans-Endothelial Invasive Ability and Cellular Motility of MDA-MB-231 Cells

Given that treatment with K100 and PTL induced spherical cluster formation of MDA-MB-231 cells in 3D cultures, thus suggesting that these cells might have a reduced ability to invade through matrigel, we sought to determine the effect of K100 *versus* PTL on the transendothelial invasive ability of these cells. For that purpose, we have used the MDA-MB-231/GFP cells having a stable expression to monitor their

invasive ability in response to treatment with K100 *versus* PTL. These later cells were transfected with an "empty" pEGFP-N1 plasmid containing only EGFP and served as a sham control for transfection in previous studies performed in our lab. In fact, the sham transfected cells as represented previously (Talhouk *et al*., 2012, submitted) have similar morphologies and growth in 2D (not shown) and 3D cultures (Figure 18A).As such equal number of untreated MDA-MB-231/GFP as well as MDA-MB-231/GFP previously treated for 24 hrs with either 5 μM PTL, 5 μM K100 or 10μM K100 were seeded over trans-well filters (having pores of 8 μm in diameter) coated with growth factor reduced matrigelcomponents and having a uniform layer of endothelial cells. Cell counting of extravasated cells after 16hrs showed that cells treated with 5 or 10μM K100 *versus* 5μM PTL exhibited reduced invasive ability by 31%, 53% and 45%, respectively (Figure 18B,C).

Furthermore, to assess whether treatment with K100 *versus* PTL affect cellular motility, a critical factor in extravasation, we performed transwell motility assays by seeding equal numbers of untreated MDA-MB-231 cells over trans-well filters (having pores of 8 μm in diameter) coated with growth factor reduced matrigel components. Cells were then treated with either 5μM PTL, 5μM K100 or 10μM K100 for 16hrs and migration through basement membrane components was then checked compared to untreated cells. Treatment with 5 or 10μM K100 *versus* 5μM PTL decreased cellular motility by 37%, 53% and 56%, respectively (Figure 18D,E).

A-

B -

| CT | 5µM PTL | 5µM K100 |

100µm

C -

10µM K100
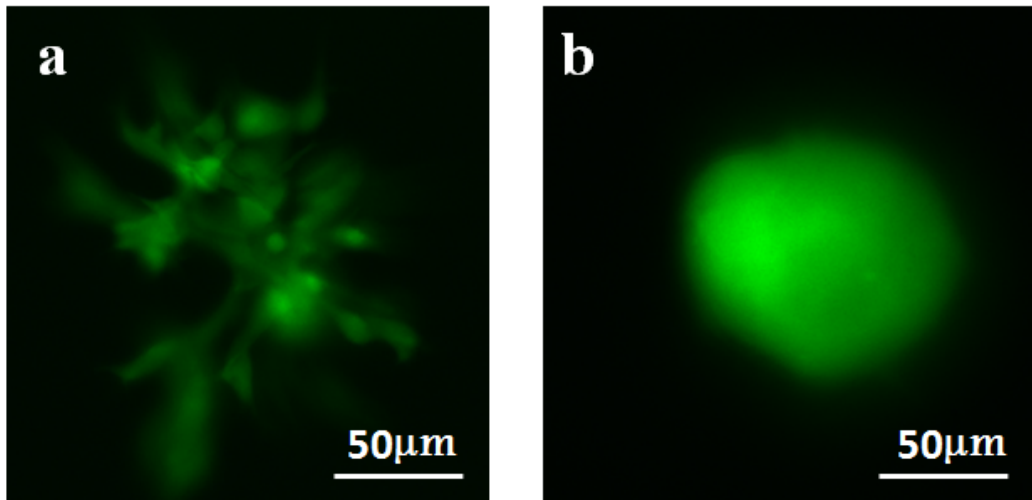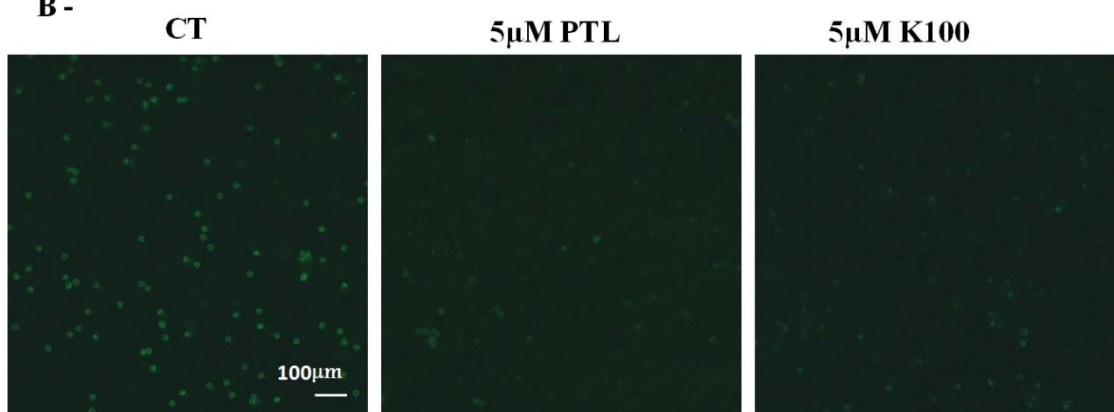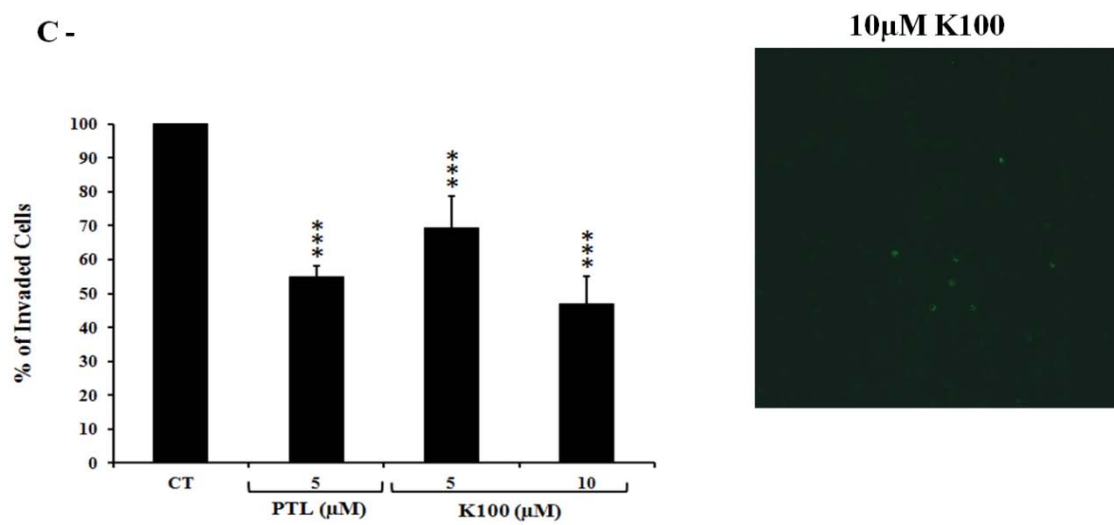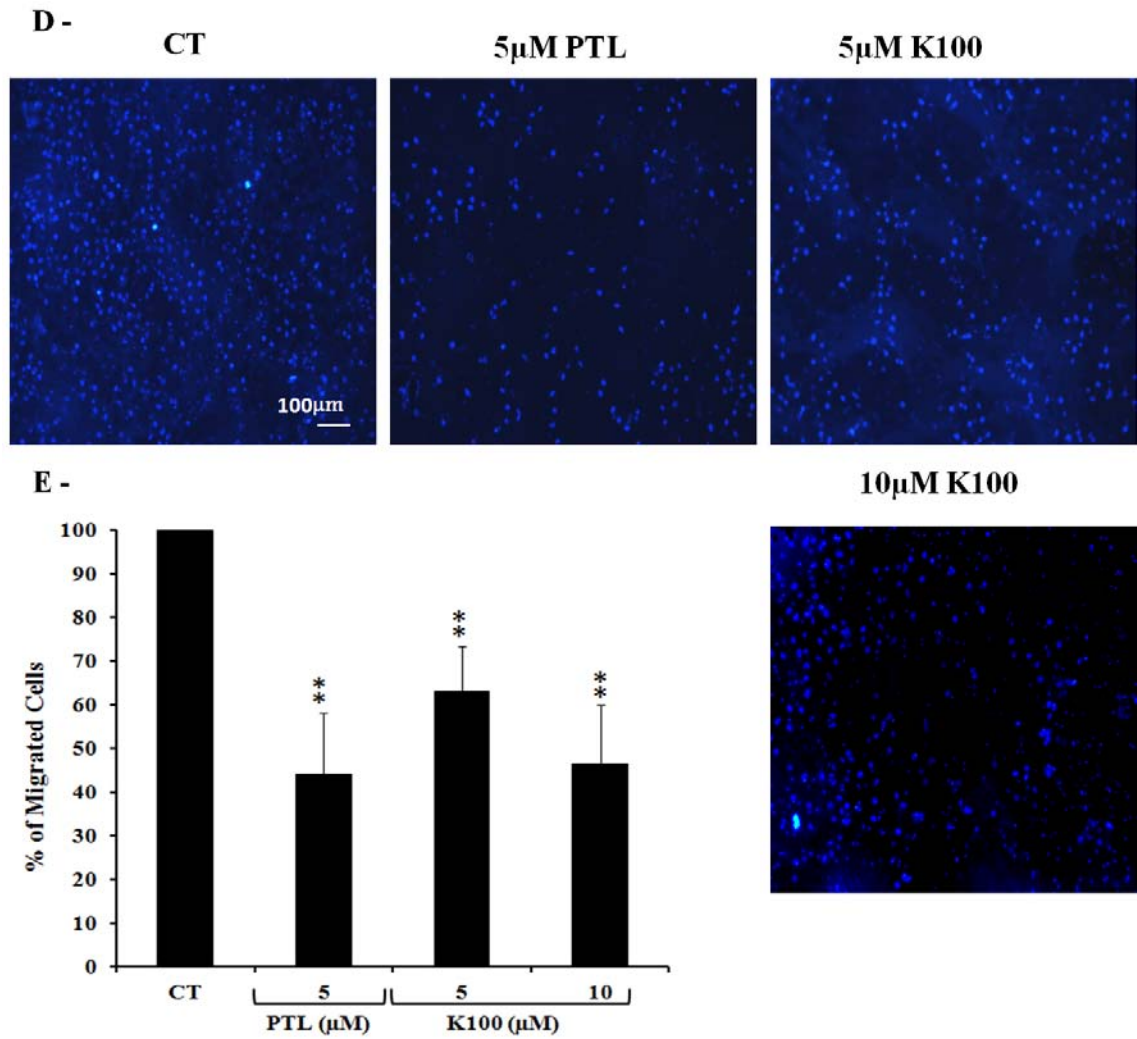
Figure 19. Effect of K100 *versus* PTL on the invasiveness and motility of MDA-MB-231 cells. (A) Fluorescent pictures of MDA-MB-231/GFP (a,b) showing stellate colonies (a) of untreated cells and spherical colonies (b) obtained upon treatment with K100 *versus* PTL. (B) Fluorescent pictures for MDA-MB-231/GFP cells showing untreated cells *versus* others treated with K100 *versus* PTL that have invaded the ECVs monolayer. (C) Histogram showing percentage of untreated invading cells *versus* others treated with K100 *versus* PTL. (D) Representative fluorescent pictures showing untreated cells *versus* others treated with K100 *versus* PTL stained with a DNA specific dye (Hoechst 33342) after migrating through matrigel and filters of 8 μm pore size. (E) Histogram showing percentage of untreated migrating cells *versus* others treated with K100 *versus* PTL. Reults represent the averages ± SD of three independent experiments. Statistical significance is represented by (***) asterisk indicating significant difference at $p<0.001$, (**) asterisk indicating significant difference at $p<0.01$ and (*) asterisk indicating significant difference at $p<0.05$.

I. K100 and PTL UP-Regulate the levels of Cadherins but Do Not Affect the Levels of P65 and MMP9

Given that K100 as well as PTL inhibited the proliferation of MDA-MB-231 cells in 2D and 3D cultures and decreased the motility and invasiveness of these cells, we sought to determine the effect of K100 *versus* PTL on the expression of several protein targets known to be important in regulating these key cellular mechanisms. The levels of pan-cadherins, major cell-cell adhesion molecules that has been shown to be strongly implicated in cancer cell invasion and metastasis regulation were assessed. Interestingly, western blotting of total cell extracts showed that treatment with 10μM K100 *versus* 5μM PTL for 24 hrs up-regulated the levels of total cadherin proteins in 2D cultures of MDA-MB-231 cells (Figure 19A). On the other hand, western blot analysis of total extracts probed with antibody against MMP9 showed that the overall levels of this protein was not altered in MDA-MB-231 cells treated with K100 *versus* PTL (Figure 19B). Moreover, treatment with K100 *versus* PTL had no effect on the total and the nuclear levels of P65 which is known to control the expression of multiple proteins involved in cell proliferation and invasiveness (Figure 19C).

A-
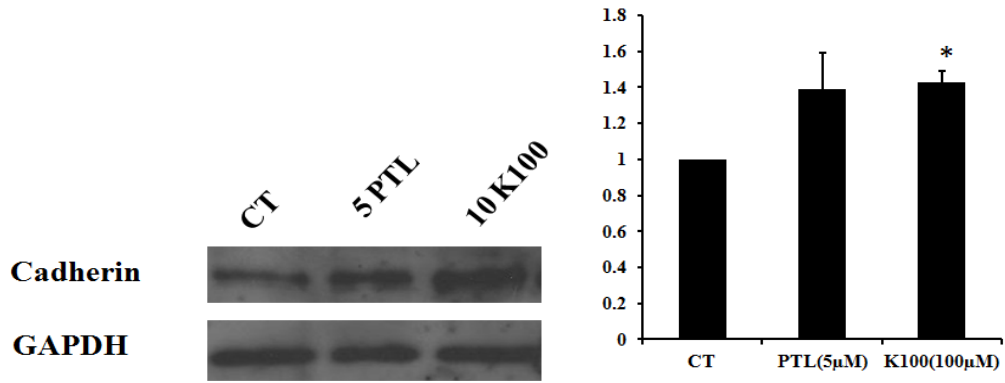
B-
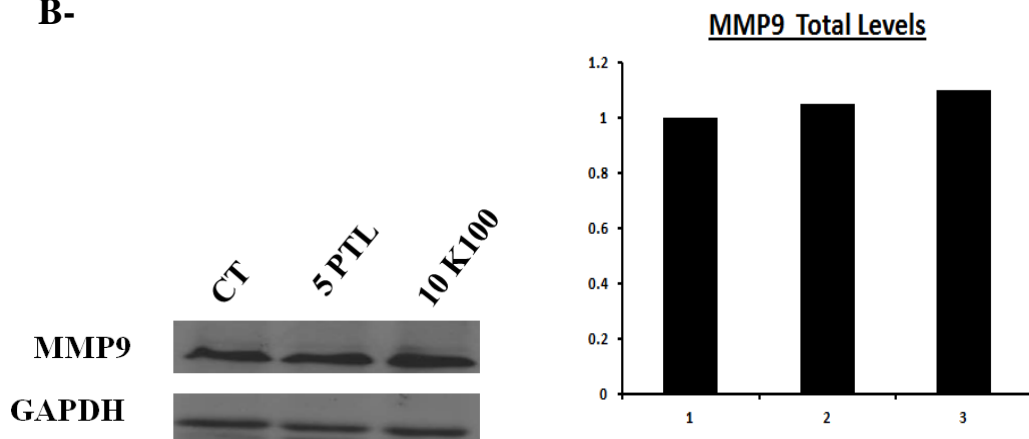
C-
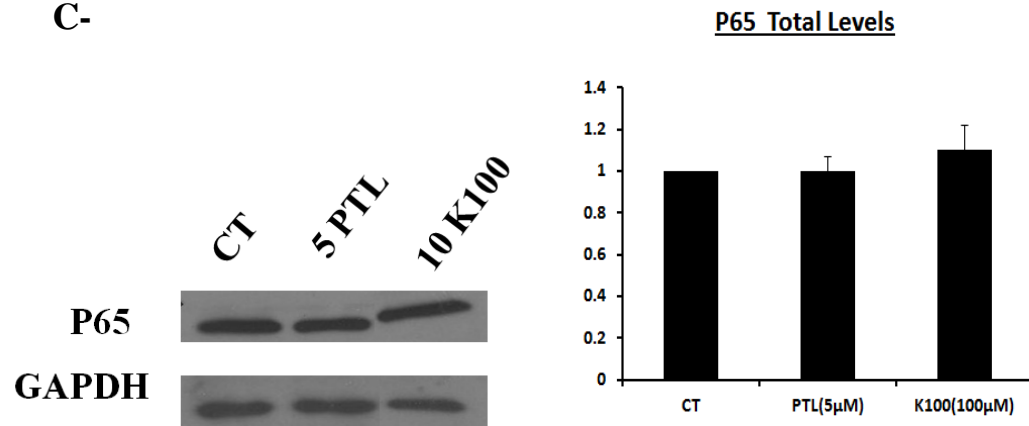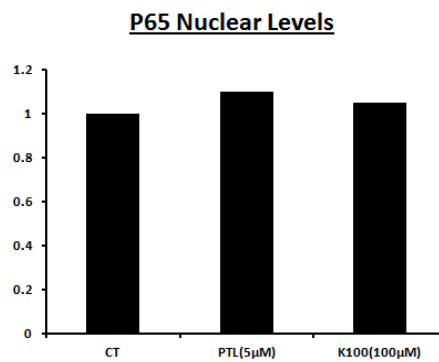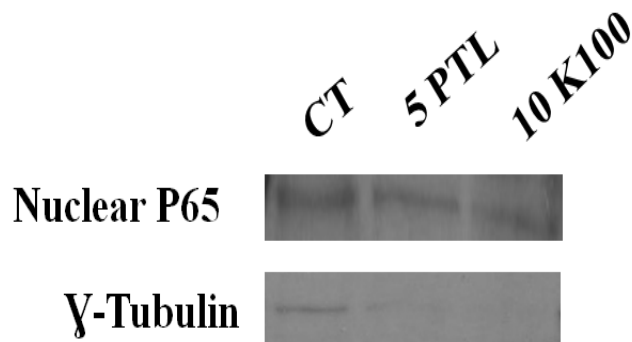
Figure 20. Effect of treatment of K100 *versus* PTL on the expression levels of several key proteins. (**A**) Western blot showing expression of PAN-cadherins in 2D-cultures of MDA-MB-231 upon treatment with 10μM K100 *versus* 5μM PTL.(B) Western Blot showing expression of MMP9in 2D-cultures of MDA-MB-231 as assessed by one experiment upon treatment with 10μM K100 *versus* 5μM PTL. (C) Western blots showing total and nuclear levels of P65 in 2D cultures of MDA-MB-231 cells upon treatment with 10μM K100 *versus* 5μM PTL. γ-Tubulin serves as a control for cytoplasmic contamination. GAPDH demonstrates equal protein loading.

61

CHAPTER IV

DISCUSSSION

Biologically active natural products extracted from medicinal plants have been recognized as being part of folk medicine for centuries. In recent years, drug discovery from medicinal plants has been the focus of extensive research where numerous studies were conducted to assess the anti-tumor as well as the anti-inflammatory activities in plants (Harvey *et al*., 2010; Greenlee, 2012). In this study, we report, for the first time, the existence of anti-tumor activities in Cota palaestina (= Anthemis palaestina ssp. syriaca), an Eastern Mediterranean endemic known in Arabic as 'Bahar ghishai'. Previous studies from our laboratory have screened for bioactive natural products with anti-inflammatory effects in a large number of selected plants endemic to the whole mediteranean basin including Lebanon (Barbour *et al*., 2004; Talhouk *et al.,* 2008). Anthemis Scariosa, now known as Cota palaestina spp.syriaca after the recognition of Cota as an independent genus (Greuter *et al*., 2003; Oberprieler *et al*., 2007 and Lo Presti *et al*., 2010), was selected among 27 other indigenous Lebanese wild plant species that have been commonly used in Lebanese folk medicine in order to study their biological activity and identify their bioactive chemical constituents. The water and methanol extracts of the aerial parts of this plant were screened for their antimicrobial (Barbour *et al.* 2004) and anti-inflammatory activities (El Jouni Thesis, 2003) and showed an efficacious inhibitory effect in both.The bioactive molecule mediating these effects, K100, was identified through bioactive-guided fractionation (Ajeeb Thesis, 2010). Chemical fractionation of the water and methanol extracts of the Cota Palestina was based on the ability of the different fractions to modulate the levels of IL-6, established in our laboratory as a marker for endotoxin (ET)-induced inflammation in

vitro (Safieh-Garabedian *et al.*, 2004), produced by ET-treated SCp2 cells. This was followed by further fractionation using column chromatography resulting in the identification of the pure compound, K100, a sesquiterpene lactone that retained the inhibition of ET-induced IL-6 production, and in a dose-dependent manner. Nuclear magnetic resonance (NMR) and Fourier transform infrared (FTIR) spectroscopy were used to elucidate the structure of the pure compound, K100. Spectroscopic data confirmed that the germacranolide 1β,10α-Epoxy-6α-hydroxy-1,10H-inunolide (K100) is isolated and identified as an anti-inflammatory compound for the first time in Cota palaestina (Talhouk and Saliba*et al.*, unpublished data). Structural analysis of K100 as well as literature reports on similar compounds(Bohlmann *et al*., 1982; Konstantinopoulou *et al*., 2003) has revealed that this molecule has four possible isomers taking into consideration the *cis* and *trans* confirmations of the two chiral centers at C7 and C8 positions (personal communication, Dr. Tarek Ghaddar). Interestingly, characterizitaion of K100 and the chemical groups mediating its bioactivities showed that the structure of K100 is analogous to that of PTL (Talhouk and Saliba*et al*., unpublished data), the major SL extracted from feverfew (Pareek *et al*., 2011). In fact, K100 bear similar functional goups to those found in PTL, namely an exocyclic α-methylene-γ-lactone ring and an epoxide moiety(Talhouk and Saliba*et al*., unpublished data). Nevertheless, K100 has an additional OH group adjacent to the α-methylene which is thought to increase its solubility and enhance its activity.

In this study, we aim to address whether K100 exhibits PTL analogous anti-cancerous activitiesthrough a comparative study for the effects of non-cytotoxic concentrations of K100 *versus* PTL on the tumor phenotype of the highly invasive mammary epithelial tumor cell line MDA-MB-231. We propose that K100 has

antitumor activities similar to those of PTL and these activities are exhibited through PTL-analogous physiological mechanisms. This hypothesis is based on a previous study conducted in our laboratory that aimed at establishing the cytotoxic profile of K100 *versus* PTL on normal (MCF-10A) and cancerous (MCF-7 and MDA-MB-231) mammary epithelial cells. This study has shown that both K100 and PTL inhibit the growth of the two cancerous cell lines in a dose dependent manner, and at concentrations tolerable by normal cells (Fares MB. Thesis Appendix, 2010). Accordingly, we set to determine the effects of non-cytotoxic concentrations of K100 *versus* PTL on cellular proliferation, motility, invasiveness and morphology of MDA-MB-231 in 3D cultures as well as to characterize their effects on the expression of key mesenchymal and metastatic markers.

Taking into consideration the homology in structure between K100 and PTL and based on the previous results in our laboratory showing PTL-analogous anti-proliferative effects of K100, we initiated our study by performing a bioinformatics molecular docking analysis *in silico* to assess the ability of K100 to bind to PTL targets such as the TNFα receptor, IKKb, the NFκB subunit P65, and members of the STAT signaling pathway (Pajak *et al*., 2008). Molecular docking is a simulation method that predicts the confirmation and binding affinity of a receptor-ligand complex (Vianna and Azevedo, 2012). As such, molecular docking simulation is perceived as a helpful computational approach in the drug-discovery process (Peitsch, 2004). Moreover, molecular docking simulations have been used by numerous studies as a tool for the design of new drugs as well as for testing the ability of potential drugs to bind key protein targets involved in various diseases such as cancer and tuberculosis (Cassidy and Setzer, 2010; Vianna and Azevedo, 2012). In order to increase the analytical

efficacy of the docking analysis, two other SLs variants (SAL A and DMAPT) were included. This study indicated that K100 is capable of binding to similar PTL protein targets with a comparable binding affinity. In fact, the values showing the lowest docking energies that reflect the strongest binding affinities clearly indicate that the binding affinities of K100 to PTL targets are very close to those of PTL indicating that the four K100 isomers can bind to PTL protein targets with a similar affinity to that of PTL. Despite being predictive, these results further confirm the structural homology between PTL and K100 and indicate that the hypothesized physiological effects of K100 could be exhibited via pathways similar to those utilized by PTL.

Studies on the plant kingdom have shown that a wide range of plants possess biologically active molecules of medicinal value and a large number of these molecules are used in the treatment of inflammation-related ailments as part of folk medicine (Talhouk *et al*., 2007). In order to confirm the anti-inflammatory effect of K100, we proceeded to check the effect of K100 on the previously assessed IL-6 levels as well as on other inflammatory mediators mainly MMP2, MMP9 and NO. As such, K100 anti-inflammatory activities were evaluated employing an *in vitro* model of endotoxin (ET)-induced inflammation in mammary epithelial SCp2 cells. Several studies on plant extracts have shown an inhibitory effect for diverse plant secondary metabolites, namely terpenoids and phenols against IL-6, NO and MMPs production (Jin *et al*., 2002; Jang *et al*., 2003). Our results show that treatment with K100 resultedin a dose-dependent down-regulation of ET-induced IL-6, MMP9 and NO production in SCp2 cells. MMP2 is abundantly produced in ET-treated and untreated cultures of SCp2 cells; nevertheless, a partial inhibition was observed at higher concentrations of K100. In fact, the ability of K100 to inhibit ET- induced cytokine IL-6, MMP-9 and NO, all common mediators of

cancer and inflammation (Schafer and Brugge, 2007) and markers of dedifferentiation (Maalouf *et al*., 2010), further confirmed K100's ant-inflammatory activities and provided an initial insight regarding its bioactivities.

Next we determined the effect of K100 *versus* PTL on the proliferation rate of the MDA-MB-231 cell line in 2D cultures. Previous studies have shown that PTL is capable of suppressing the proliferation and inducing apoptosis in many human cancer cells *in vitro*, such as hepatoma, human lung carcinoma (A549), human medulloblastoma (TE671), cholangiocarcinoma, colorectal and pancreatic cancers (Zhang *et al*. 2004; Parada *et al*. 2007; Kim *et al*. 2005; Pajak *et al*., 2008). Furthermore, other reports have shown that PTL can specifically eradicate malignant cells, such action was addressed by Guzman *et al*. (2009) who showed that PTL preferentially targets leukemia stem cells while sparing normal hematopoetic stem cells. Also a recent study have shown that PTL showed a considerable cytotoxicity against breast cancer MDA-MB-231 and MCF-7 adenocarcinoma cells at ~ 9µM concentration. Previous results from our laboratory have shown that K100 is less cytotoxicity than PTL inhibiting the growth of two mammary epithelial tumor cell lines in a dose dependent manner, at concentrations tolerable by normal cell lines. Moreover, when compared to PTL, K100 exhibited a larger difference between concentrations affecting cancerous but not normal cells (Fares MB. Thesis Appendix, 2010). In line with these data, our data show that K100 inhibited the growth of MDA-MB-231cells in a dose dependent manner and at non-cytotoxic concentrations (10 & 20µM). On the other hand, PTL also inhibited the growth of MDA-MB-231 cells at a 5µM concentration; nonetheless it was highly toxic at a 20µM concentration. Interestingly when compared to PTL, K100

exhibited a larger difference between concentrations affecting cancerous but not normal cells (Fares MB. Thesis Appendix, 2010).

Several SLs have been shown to disrupt cell cycle progression in various types of cancer cells (Zhang *et al*., 2005). One of these SLs, PTL, has been reported to cause cell cycle progression arrest at the G2/M check point in the sarcomatoid hepatocellular carcinoma cell line (SH-J1) and at the G1 phase in the human 5637 bladder cancer cells and at G1/S pahse at various leukocyte cancer cell lines (Cheng *et al.* 2011; Cho *et al*., 2004). Taking into consideration these studies and that K100 and PTL decreased the proliferation rate of MDA-MB-231 at non-cytotoxic concentrations (10μM K100, 5μM PTL) we assessed the effect of these concentrations on cell cycle progression of MDA-MB-231 cells grown under 2D culture conditions. Interestingly, in this study we show that this decrease in cell proliferation was accompanied by a 54% prolongation of S-phase of the cell cycle in cells treated with 10μM K100 compared to a 74% prolongation in cells treated with 5μM PTL. Nevertheless, it was until recently that basic research testing the efficacy of novel anticancer drugs was performed on cells grown on two-dimensional (2D) glass or plastic platforms; however, an emerging view finds that traditional 2D cell culture may not accurately mimic the three-dimensional (3D) environment in which cancer cells reside (Gurski *et al*., 2010). More specifically, the unnatural 2D environment may provide inaccurate data regarding the predicted response of cancer cells to chemotherapeutics where it is now known that signaling pathways that are crucial in cancer cells and are the drug targets behave differently in 3D and 2D and, thus, drug testing must be done also in 3D culture.Moreover, other striking differences including morphology and growth of cancerous cells are noticed when comparing 2D and 3D cultures (Bissell *et al.* 2002). For this reason, there is now

considerable interest in developing 3D *in vitro* systems for testing the efficacy of anti-cancer drugs (Gurski *et al*., 2010).As such, we sought to check the effect of K100 *versus* PTL on the growth and proliferation of MDA-MB-231 cells under these culture conditions. Interestingly, both K100 and PTL significantly decreased the proliferation rate of MDA-MB-231 cells grown in 3D cultures without inducing their death. It is essential to note that both K100 as well as PTL did not result in a significant difference in cell death among treated and untreated cells. This is important as both K100 and PTL were shown to be cytotoxic in 2D cultures at concentrations greater than 10 and 20μM respectively. This data is in line with previous studies showing that culture in 3D matrices desensitize cancer cells to drug treatments (Serebriiski *et al*., 2008). Cells grown in 3D are more resistant to chemotherapy than those grown in 2D cultures and studies suggest important rolesfor cellular architecture, phenotypic variations and extracellular matrix barrier to drug transport in drug efficacy (Horninq *et al*., 2008). Moreover, it has been shown that small molecules including drugs could bind to proteins found in matrigel such as collagen and laminin therby decreasing the cytotoxic effects of these drugs on cells cultured on 3D matrices (Zhang *et al*., 2006). While both untreated MDA-MB-231 cells as well as those treated with K100 *versus* PTL grow similarly in monolayers in 2D cultures, their morphology was significantly different when grown in 3D culture systems. Indeed, untreated MDA-MB-231 cells formed stellate colonies upon adhering to the growth factor-reduced EHS (Matrigel), which is typical of MDA-MB-231 malignant cells (Kenny *et al*., 2007). In contrast, cells treated with K100 *versus* PTL grew into spherical colonies unlike that of cancer cells. K100 resulted in a more significant shift of MDA-MB-231 cells morphology in 3D compared to PTL.Moreover, cells treated with K100 demonstrated a dominance of smaller sized

colonies when compared to untreated cells, while cells treated with PTL showed a dominance of medium colonies instead of small ones. Hence, suggesting that the malignant invasive phenotype of these cells might be reversed. This decrease in colony size can be correlated to the reduced proliferation rate of cells treated with K100 *versus* PTL. Based on this shifting of morphology from stellate to spherical upon treatment with K100 and PTL, it will be interesting in the future to check whether treatment with K100 *versus* PTL for longer periods could revert the morphology of MDA-MB-231 cells into a morphology similar to that of normal mammary epithelial cells that are generally able to form a differentiated unit structure in 3D conditions that recapitulate many aspects of glandular mammary architecture in vivo (Shaw *et al.*, 2007). Therfore, inducing a mesenchymal to epithelial transition through forming polarized acini-like spheroids with a lumen. PTL has been reported to inhibit the invasiveness and migration of BxPC-3 pancreatic cancer cells (Liu *et al*., 2010) and reduce the metastasis of MDA-MB-231 cells in a xenograft model of breast cancer in combination with docetaxel (Sweeney *et al*., 2005). Therefore, we sought to determine the effect of K100 *versus* PTL on the motility and invasive ability of MDA-MB-231 cells. For that purpose, we have used the MDA-MB-231/GFP cells having a stable expression of GFP to monitor their invasive ability in response to treatment with K100 *versus* PTL. These were transfected with an "empty" pEGFP-N1 plasmid containing only EGFP and served as a mock control for transfection in previous studies performed in our lab (Talhouk *et al*., 2012, submitted). The sham transfected cells have similar morphologies and growth rates in 2D and 3D cultures when compared to untransfected cells (Talhouk *et al*., 2012, submitted). Our results show that treatment with K100 *versus* PTL reduced the ability of MDA-MB-231 cells to extravasate through the endothelial cells and basement

membrane components by approximately 50%. In another study PTL has been shown to have an anti-migratory effect on breast cancer MCF-7 cells (Wyrebska *et al*., 2012). In line with these results, our results reveal that cellular motility, a critical step in metastasis, was also reduced by more than 50% upon treatment with K100 *versus* PTL.

As an initial insight into the mechanism mediating this anti-cancerous effect by K100 *versus* PTL, we sought to determine the effect of K100 *versus* PTL on the expression levels of several protein targets including MMP9, P-65 and cadherins. There is now sufficient evidence that NF-kB is the main molecular target for several SLs such as PTL and helanin (Zhang *et al*. 2005; Ghantous *et al*., 2010).In addition, recent reports have shown that NF-kB induces the expression of MMPs and cytokines in highly invasive breast cancer cell lines (Helbig *et al*. 2003). Moreover, it has been recently shown that PTL suppresses mRNA levelof MMP9 and VEGF in melanoma cells (A375) (Czyz *et al.* 2010) and osteosarcoma cell line LM8 respectively (Kishida *et al*. 2007). Our results show that treatment with K100 *versus* PTL had no effect the total and nuclear levels of P65 as well as the total expression levels of MMP9 in 2D cultures of MDA-MB-231. As these results were common between PTL and K100 and contradictory to reported literarture, it might be that increasing the concentration and period of treatment of both drugs could result in the inhibition of NF-kB and its downstream targets and thus lower the expression levels of P65. Moreover, our results show a small band of nuclear P65 which might be due to cytoplasmic contamination as shown by γ-tubulin levels and thus are not conclusive. Therefore, it would be interesting to check the effect of K100 *versus* PTL on the activity of NF-kB through electrophoretic mobility shift assay (EMSA). Several studies have shown cadherins to be implicated in cancer cells invasion and metastasis regulation (Jeans *et al*., 2008; Takeichi, 1993), yet

no studies have shown the effect of plant-derived natural products on cadherins expression levels. Taking into account the anti-invasive abilities of PTL and K100, we sought to assess the levels of pan-cadherins in 2D cultures of MDA-MB-231 cells upon treatment with K100 *versus* PTL. Studies have shown that P and N cadherin exhibit various roles by either promoting adhesion or inductingmigration depending on the cellular context. Our results show ~50% increase in cadherins expression levels in cells treated with K100 and PTL compared to control cells. In line with studies showing that upregulation of either E or P cadherin in MDA-MB-231 cells decreased the invasiveness and migration, our results show an upregulation in cadherins expression associated with a decrease in invasiveness and migration of MDA-MB-231 cells upon treatment with K100 and PTL (Sarrio *et al*., 2009). We speculate that this increase in cadherins levels is due to an increase in P and E cadherins which are both implicated in MET suggesting that K100 *versus* PTL might be inducing a partial MET which would be further addressed in our future studies.

In conclusion, our results show that K100 exhibits a potent anti-inflammatory effect by inhibiting the ET-induced production of several markers of inflammation, namely IL-6, MMP9 and NO. Moreover, our data shows that K100 is capable of binding to PTL protein targets at similar positions and with a similar affinity. We show that K100 and PTL inhibited the proliferation and prolonged the S-phase of MDA-MB-231 cells in 2D cultures. Also, K100 and PTL inhibited the growth and induced a shift in the morphology of MDA-MB-231 cells from stellate to spherical in 3D cultures associated with a decrease in the size of colonies. Interestingly, K100 and PTL significantly inhibited the invasion and motility of MDA-MB-231 cells. This study suggests a comparable effect for K100 and PTL on the tumor phenotype of MDA-MB-

231 cells. Moreover, these data and previous data from our laboratory suggests several advantages for K100 over PTL in terms of possibility for having higher solubility, a wider range of concentrations affecting cancer cells but not normal ones and its ability to induce a gain of function through increasing the expression of cadherins and β-casein levels. Therefore, K100 can be perceived as a promising anti-inflammatory and anti-tumor molecule and proposed for further investigations through *in vivo* studies.

REFERENCES

Acamovic, T. and Brooker, J.D. (2005). Symposium on 'Plants as animal foods: a case of catch 22?' Biochemistry of Plant Secondary Metabolites and Their Effects in Animals.*Proceedings of the Nutrition Society.*64, 403-412.

Barbour, E. K., Al Sharif, M., Sagherian, V. K., Habre, A. N., Talhouk, R. and Talhouk, S. N. (2004). Screening of selected indigenous plants of Lebanon for antimicrobial activity. *J. Ethnopharmacol*. 93, 1-7.

Bissell, M., Radisky, D., Rizki, A., Weaver, V. and Petersen, O. 2002. The organizing principle: microenvironmental influences in the normal and malignant breast. *Differentiation*. 70, 537–546.

Bohlmann, F., Adler, A., Jakupovic, J., King, R. M. and Robinson, H. (1982).A dimeric germacranolide and other sesquiterpene lactones from Mikania species.*Phytochemistry*. 21, 1349-1355.

Buijs, J., Henriquez, N., Van Overveld, P., Van der Horst, G., Que, I., Schwaninger, R., Rentsch, C., Ten Dijke, P., Cleton-Jansen, A., Driouch, K., Lidereau, R., Bachelier, R., Vukicevic, S., Clézardin, P., Papapoulos, S., Cecchini, M., Löwik, C. and Van der Pluijm, G. (2007). *Cancer Res*. 06, 2490.

Burdall, S., Hanby, A., Lansdown, M. and Speirs, V. (2002). Breast Cancer Cell lines: friend or foe? *Breast Cancer Res*. 5, 89-95.

Cassidy, C. and Setzer, N. (2010). Cancer-relevant biochemical targets of cytotoxic *Lonchocarpus* flavonoids: A molecular docking analysis. *J.Mol Model*. 16, 311-326.

Çelik, S., Rosselli, S., Maggio, A., Raccuglia, R. A., Uysal, I., Kisiel, W. and Bruno, M. (2005). Sesquiterpene lactones form Anthemis wiedemanniana. *Biochem Syst Ecol*. 33, 952-956.

Chao, Y., Shepard, C. and Wells, A. (2010). Breast carcinoma cells re-express E-cadherin during mesenchymal to epithelial reverting transition. *Mol Cancer*. 9-179.

Chaturvedi, D. (2011). Sesquiterpene lactones: Structural diversity and their biological activities. *Opportunity, Challenge and Scope of Natural Products in Medicinal Chemistry*. 313-334.

Cheng, G. and Xie, L. (2011). Parthenolide Induces Apoptosis and Cell Cycle Arrest of Human 5637 Bladder Cancer Cells In Vitro. *Molecules.* 16, 6758-6768.

Choi, J. H., Ha J., Park, J.H., Lee, J.Y., Lee, Y.S., Park, H.J., Choi, J.W., Masuda, Y Nakaya, K. and Lee, K.T. (2002).*J. Cancer Res*. 93-1327.

Cragg, G. and Newman, D. (2005). Plants as a source of anti-cancer agents.*Journal of enthnopharmacology.*100, 72-79.

Czyz, M., Lesiak-Mieczkowska, K., Koprowska, K., Szulawska-Mroczek, A. and Wozniak, M. (2010). Cell context-dependent activities of parthenolide in primary and metastatic melanoma cells. *British Journal of Pharmacology*. 160, 1144-1157.

Da Costa, F. B. , Terfloth, L. and Gasteiger, J. (2005). Sesquiterpene lactone-based classification of three Asteraceae tribes: a study based on self-organizing neural networks applied to chemosystematics. *Phytochemistry*. 66, 345-353.

Dai, J. and Mumper, R. J. (2010) Plant Phenolics: Extraction, Analysis and Their Antioxidant and Anticancer Properties. *Molecules*. 15, 7313-7352.

Das, S, Becker, B., Hoffmann, F. and Mertz, J. (2009). Complete reversal of epithelial to mesenchymal transition requires inhibition of both ZEB expression and the Rho pathway. *BMC Cell Biol*. 10-94.

De Sampaio, P., Auslaender, D., Krubasik, D., Failla, A., Skepper, J., Murphy, G. and English, W. (2012). A Heterogeneous InVitro Three Dimensional Model of Tumour-Stroma Interactions Regulating Sprouting Angiogenesis.*PLoS ONE*. 7(2), e30753.

Devik Gunasinghe, A., Wells, A., Thompson, E. and Hugo, H. (2012). Mesenchymal–epithelial transition (MET) as a mechanism for metastatic colonisation in breast cancer. *Cancer Metastasis Rev*. 012, 9377-5.

Drasin, D., Tyler, R. and Ford, H. (2011). Breast cancer epithelial-to-mesenchymal transition: examining the functional consequences of plasticity. *Breast Cancer Research*.13, 226.

Dykxhoorn, D., Wu, Y., Xie, H., Yu, F., Lal, A. and Petrocca, F. (2009).miR-200 enhances mouse breast cancer cell colonization to form distant metastases. *PLoS ONE*. 4(9), e7181.

Efferth, T. Cancer Therapy with Natural Products and Medicinal Plants. (2010). *Planta Med*. 76, 1035-1036.

Gao, D., Joshi, N., Choi, H., Ryu, S., Hahn, M., Catena, R., Sadik, H., Argani, P., Wagner, P., Vahdat, L., Port, J., Stiles, B., Sukumar, S., Altorki, N., Rafii, S. and Mittal, V. (2012).Bone marrow-derived myeloid progenitor cells promote metastases by induction of mesenchymal to epithelial transition*Cancer Res*. 11, 2905.

Ghantous, A., Gali-Muhtasib, H., Vuorela, H., Saliba, N. and Darwiche, N. (2010). What made sesquiterpe ne lac tones reach cancer clinical trials? *Drug Discovery Today*.15 Numbers 15/16.

Godde, N., Galea, R., Elsum, I. and Humbert, P. (2010). Cell Polarity in Motion: Redefining Mammary Tissue Organization Through EMT and Cell Polarity Transitions. *J Mammary Gland Biol Neoplasia*. 15, 149–168.

Greenlee, H.(2012). Natural products for cancer prevention.*Seminars in oncology nursing*. 28, 29-44.

Greuter, W., Oberprieler, C. and Vogt, R. (2003). The Euro+Med treatment of Anthemideae (Compositae) – generic concepts and required new names.*Willdenowia - Annals of the Botanic Garden and Botanical Museum Berlin-Dahlem*. 33, 37-43.

Gunasinghe, N., Wells, A., Thompson, E. and Hugo, H. (2012). Mesenchymal–epithelial transition (MET) as a mechanism for metastatic colonisation in breast cancer. *Cancer and Metastasis Reviews*, 1-10.

Gurib-Fakim, A. (2006). Medicinal Plants: Traditions of Yesterday and Drugs of Tomorrow. *Molecular aspects of Medicine*. 27, 1-93.

Gurski, L., Petrelli, N., Jia, X., Farach-Carson, M. (2010). 3D matrices for anti-cancer drug testing and development.*Oncology issues*. 25, 20-25.

Guzman, M. L., Neelakantan, S., Nasim, S., Jordan, C.T.; Crooks, P. A. (2009). Aminoparthenolides as novel anti-leukemic agents: Discovery of the NFKB inhibitor, DMAPT (lc-1). *Bioorg. Med. Chem. Lett*. 19, 4346-4349.

Guzman, M. L., Rossi, R. M., Neelakantan, S., Li, X., Corbett, C. A., Hassane, D. C., Becker, M. W., Bennett, J. M., Sullivan, E., Lachowicz, J. L., Vaughan, A., Sweeney, C. J., Matthews, W., Carroll, M., Liesveld, J. L., Crooks, P. A., Jordan, C. T. (2007). An orally bioavailable parthenolide analog selectively eradicates acute myelogenous leukemia stem and progenitor cells. *Blood*. 110, 4427-4435.

Harvey, A. and Cree, I.(2010). High-Throughput Screening of Natural Products for Cancer Therapy.*Planta Med*. 76, 1080–1086.

Hehner SP, Hofmann TG, Droge W and Schmitz ML. (1999). The antiinflammatory sesquiterpene lactone parthenolide inhibits NF-kappa B by targeting the I kappa B kinase complex. *J. Immunol*. 163, 5617–562.

Helbig, G., Christopherson, K., Bhat-Nakshatri, P., Kumar, S., Kishimoto, H., Miller, K., Broxmeyer, H.and Nakshatri, H. (2003). NF-kB Promotes Breast Cancer Cell Migration and Metastasis by Inducing the Expression of the Chemokine Receptor CXCR4. *The Journal of Biological Chemistry*. 21631–21638.

Heldt, H. and Heldt, F. (2012). Secondary metabolites fulfill specific ecological functions in plants. *Plant Growth Regulation*. 26, 399-408.

Heppner, G., Miller, F. and Shekhar, P. (2000). Nontransgenic models of breast cancer. *Breast Cancer Research*. *2*, 331-334.

Holliday, D. and Speirs, V. (2011). Choosing the right cell for breast cancer research. *Breast Cancer Res*. 13-215.

Horning,J., Sahoo, S., Vijayaraghavalu, S., Dimitrijevic,S., Vasir, J., Jain, T., Panda, A.and Labhasetwar, V.(2008). 3-D Tumor Model for *In Vitro* Evaluation of Anticancer Drugs. *Molecular pharmaceutics*. 5, 849-862.

Hsu, Y., Ling-Yu, W. and Po-Lin, K. (2009). Dehydrocostuslactone, a Medicinal Plant-DerivedSesquiterpene Lactone, Induces Apoptosis Coupled to Endoplasmic Reticulum Stress in Liver Cancer Cells. *The Journal of Pharmacology and Experimental Therapeutics*. 329, 808-819.

Huang W., Yi-Zhong C. and Zhang, Y. (2009).Natural Phenolic Compounds From Medicinal Herbs andDietary Plants: Potential Use for Cancer Prevention. *Nutrition and Cancer*. 62:1, 1-20.

Hurteau, G., Carlson, J., Spivack, S. and Brock, G. (2007). Overexpression of the microRNA hsa-miR-200c leads to reduced expression of transcription factor 8 and increased expression of E-cadherin. *Cancer Res*. 67, 7972–6.

Iorns, E., Clarke, J., Ward, T., Dean, S. and Lippman, M. (2012). Simultaneous analysis of tumor and stromal gene expression profiles from xenograft models. *Breast Cancer Res Treat*. 131, 321-324.

Jang, S., Jeong, S., Kim, K., Kim, H., Yu, H., Park, R., Kim, H. and YO, Y. (2003). Tanshinone IIA from *Salvia miltiorrhiza* inhibits inducible nitric oxide synthase expression and production of TNFalpha, IL-1beta and IL-6 in activated RAW 264.7 cells. *PlantaMed*. 69, 1057–1059.

Jeanes, A., Gottardi, C., and Yap, A. (2008). Cadherins and cancer: how does cadherin dysfunction promote tumor progression&quest. *Oncogene*,*27*, 6920-6929.

Jeonga, S., Itokawab, T., Shibuyac, M., Kuwanob, M., Onob, M., Higuchia, R. and Miyamoto, T. (2002). Costunolide, a sesquiterpene lactone from Saussurea lappa inhibits the VEGFR KDR/Flk-1 signaling pathway. Cancer Letters. 187, 129-133.

Jin, H., Hwang, B., Kim, H., Lee, J., Kim, Y. and Lee, J. (2002) Antiinflammatory constituents of *Celastrus orbiculatus* inhibit the NF-kappaB activation and NO production. *J Nat Prod*.65,89–91.

Kalluri, R. and Weinberg, R.A. (2009). The basics of epithelial mesenchymal transition.*J. Clin Invest*. 119, 1420–1428.

Kemper, K. Feverfew (Tanacetum parthenium). 1999.

Kenny, P., Lee, G., Myers, C., Neve, R., Semeiks, J., Spellman, P., Lorenz, K., Lee, E., Barcellos-Hoff, M., Petersen, O., Gray, J. and Bissell M. (2007). The morphologies of breast cancer cell lines in three-dimensional assays correlate with their profiles of gene expression. *Molecular oncology*. 1, 84-96.

Kim, J., Liu, L., Lee, S., Kim, Y., You K. and Kim, D. (2005). Susceptibility of cholangiocarcinoma cells to parthenolide-induced apoptosis. *Cancer Res* 65, 6312-6320.

Kishida, Y., Yoshikawa, H. and Myoui, A. (2007).Parthenolide, a Natural Inhibitor of Nuclear Factor-Kappab, Inhibits Lung Colonization of Murine Osteosarcoma Cells. *Clin Cancer Res*. 13, 59-67.

Konstantinopoulou, M., Karioti, A., Skaltsas, S., Skaltsa, H.(2003). Sesquiterpene lactones from Anthemis altissima and their anti-Helicobacter pylori activity.*J. Nat. Prod*. 66, 699-702.

Lcroix, M. and Leclercq G. (2004). Relevance of breast cancer cell lines as models for breasttumours: an update. *Breast Cancer Research and Treatment*. 83, 249–289.

Liu, J., Cai, M., Xin, Y., Wu, Q., Ma, J., Yang, P., Xie, H., Huang, D. (2010). Parthenolide induces proliferation inhibition and apoptosis of pancreatic cancer cells in vitro. *J. Exp. Clin*. Cancer Res. 29, 108.

Liu, M., and Hicklin, D. (2011).Human tumor xenograft efficacy models. *Tumor Models in Cancer Research*, 99-124.

Lo Presti, R. M. and Oberprieler, C. (2010). Evolutionary history, biogeography and eco-climatological differentiation of the genus Anthemis L. (Compositae Anthemideae) in the circum-mediterranean area.*Journal of Biogeography*. 36, 1313-1332.

Maalouf, S., Talhouk, R. and Schanbacher, F.(2010). Inflammatory responses in epithelia: endotoxin-induced IL-6 secretion and iNOS/NO production are differentially regulated in mouse mammary epithelial cells. *Journal of inflammation.*7, 58.

Merfort, I. (2011). Perspectives on Sesquiterpene Lactones in Cancer and Inflammation.*Current Drug Targets.* 12, 1560-1573.

Micalizzi, D., Farabaugh, S. and Ford, H. (2010).Epithelial-Mesenchymal Transition in Cancer Parallels Between Normal Development and Tumor Progression.*J Mammary Gland Biol Neoplasia* 15, 117–134.

Minn, A., Gupta, G., Siegal, P., D.Bos, P., Shu, W., Giri, D., Viale, A., Olshen, A., Gerald, W. and Massague J. (2005). Genes that mediate breast cancer to lung. *Nature*. 436, nature 03799.

Naishnav, P. and Demain, A. L., (2011). Unexpected applications of secondary metabolites.*Biotechnology Advances*. 29, 223-229.

Nakshatri, H., Rice, S., and Bhat-Nakshatri, P. (2004). Antitumor agent parthenolide reverses resistance of breast cancer cells to tumor necrosis factor-related apoptosis-inducing ligand through sustained activation of c-Jun N-terminal kinase. *Oncogene*. *23*, 7330-7344.

Oberprieler, C., Himmelreich, S., Källersjö, M., Vallès, J., Watson, L. E. and Vogt, R. (2009).*Anthemideae*. 631-666.

Oberprieler, C., Himmelreich, S., Vogt, R. (2007). Willdenowia. A New Subtribal Classification of the Tribe Anthemideae (Compositae). 37, 89-114.

Pajak, B., Gajkowska, B., Orzechowski, A. (2008). Molecular basis of parthenolide-dependent proapoptotic activity in cancer cells.*Folia Histochem Cytobiol*. 46(2), 129-35.

Parada-Turska, J., Paduch, R., Majdan, M., Kandefer-Szerszeñ, M. and Rzeski, W. (2007).Antiproliferative activity of parthenolide against three human cancer cell lines and human umbilical vein endothelial cells.*Pharmacological Reports*. 59, 233-237.

Pareek, A., Suthar, M., Rathore, G. and Bansal, V. (2011). Feverfew (*Tanacetum parthenium* L.): A systematic review. *Pharmacognosy review*. 5, 103-110.

Peinado, H., Portillo, F. and Cano, A. (2004). Transcriptional regulation of cadherins during development and carcinogenesis.*Int J Dev Biol*. 48, 365–75.

Peitsch, M. (2004). Manuel Peitsch discusses knowledge management and informatics in drug discovery. *Drug discovery today biocilio.* 02, 94-96.

Post, G. and Dinsmore, J. (1932).Flora of Syria, Palestine and Sinai, American Press, Beirut.

Rabi, T. and Bishayee, A. (2009). Terpenoids and breast cancer chemoprevention.*Breast Cancer Res Treat*. 115, 223-239.

Regina, M., Grootjans, S., Biavatti, M. W., Vandenabeele, P. and D'herde, Katharina. (2012). Sesquiterpene lactones as drugs with multiple targets in cancer treatment: focus on parthenolide. *Anticancer Drugs*. 23(9). 883-96.

Safieh-Garabedian, B., M., G.M., El-Jouni, W., Khattar, M. and Talhouk, R. (2004):The effect of endotoxin (ET) on functional parameters of mammary CID-9 cells in culture. *Reproduction*. 127, 397-406.

Sarker, S. D., Latif, Z. and Gray, A. I. (2009).Natural Product Isolation.*Methods in Biotechnology*. 20, 1-23.

Sarrió, D., Palacios, J., Hergueta-Redondo, M., Gómez-López, G., Cano, A. and Moreno-Bueno, G. (2009).Functional characterization of E-and P-cadherin in invasive breast cancer cells. *BMC cancer*. 74.

Schafer, Z. and Brugge, J. (2007). IL-6 involvement in epithelial cancers.*The Journal of Clinical Investigation.* 117, 3660-3663.

Serebriiskii, I., Castello-Cros, R. and Lamb, A. (2008). Fibroblast-derived 3D matrix differentially regulates the growth and drug-responsiveness of human cancer cells. *Matrix Biol.* 27, 573-585.

Sharma, H., Parihar, L. and Parihar, P. Review on cancer and anticancerous properties of some medicinal plants. *Journal of Medicinal Plants Research.* 5(10), 1818-1835.

Shaw, R., Fay, A., Puthenveedu, M., von Zastrow, M., Jan, Y.and Jan, L. (2007). Microtubule plus-end-tracking proteins target gap junctions directly from the cell interior to adherens junctions. *Cell.* 128, 547-560.

Sweeney, C., Mehrotra, S., Sadaria, M., Kumar, S., Shortle, N., Roman, Y., Sheridan, C., Campbell, R., Murry, D., Badve, S. and Nakashtri, H. (2005). The sesquiterpene lactone parthenolide in combination with docetaxel reduces metastasis and improves survival in a xenograft model of breast cancer. *Mol cancer ther.*4, 1004-1012.

Takeichi, M. (1993). Cadherins in cancer: implications for invasion and metastasis. *Current opinion in cell biology.* 5, 806-811.

Talhouk, R., El-Jouni, W., Baalbaki, R., Gali-Muhtasib, H., Kogan, J., and Talhouk, S. (2008). Anti-inflammatory bio-activities in water extract of Centaurea ainetensis. *Journal of Medicinal Plants Research.* 2 (1), 024–033.

Talhouk, R., Karam, C., Fostok, S., El-Jouni, W. and Barbour, E. (2007). Anti-inflammatory bioactivities in plant extracts. *J Med Food.* 10, 1-10.

Teixeira da Silva, J. (2004). Mining the essential oils of the Anthemideae. *Afr J Biotechnol.* 3, 706-720.

Townsend, T. A., Wrana, J. L., Davis, G. E. and Barnett, J. V. (2008). Transforming growth factor-beta-stimulated endocardial cell transformation is dependent on Par6c regulation of RhoA. *J Biol Chem.* 283, 13834–41.

Vargo-Gogola, T., Rosen, J. (2007). Modeling breast cancer: one size does not fit all, *NatRev. Cancer.* 7 (9), 659– 672.

Vasas, A. and Hohmann J. (2010). Xanthane sesquiterpenoids: structure, synthesis and biological activity. *Nat. Prod. Rep.* 28, 824-842.

Vianna, C. and de Azevedo, W. (2012). Identification of new potential *Mycobacterium tuberculosis* shikimate kinase inhibitors through molecular docking simulations. *J.Mol Model.* 18, 755-764.

Vinci, M., Gowan, S., Boxall, F., Patterson, L., Zimmermann, M., Court, W., Lomas, C., Mendiola, M., Hardisson, D. and Eccles, S. (2012). Advances in Establishment and analysis of three-dimensional tumor spheroid-based functional assays for target validation and drug evaluation.*Journal of Biology.* 10-29.

Wang, G., Tang W. and. Bidigare R. R. (2005). Natural Products: Drug Discovery and *Therapeutic Medicine*. Part 3, 197-227.

Willoughby, J., Sundar, S., Cheung, M., Tin, A., Modiano, J. and Firestone G. (2009). Artemisinin blocks prostate cancer growth and cell cycle progression by disrupting Sp1 interactions with the cyclin-dependent kinase-4 (CDK4) promoter and inhibiting CDK4 gene expression. *J Biol Chem*. 284(4), 2203-13.

Wink, M. (2004). Evolution of toxins and antinutritional factors in plants with special emphasis on Leguminosae.*Poisonous Plants and Related Toxins*. 1–25.

Wink, M. (2010). Introduction Biochemistry and Ecol.ogical Functions of Secondary Metabolites. *Annual Plant Reviews*. 40, 1-19.

Wink, M. 2004. Evolution of toxins and antinutritional factors in plants with special emphasis on Leguminosae.*In Poisonous Plants and Related Toxins*. 1–25.

Wyrebska, A., Gach, K., Szemraj, J., Szewczyk, K., Hrabec, E., Koszuk, J., Janecki, T. and Janecka, A.(2012). Comparison of anti-invasive activity of parthenolide and 3-isopropyl-2-methyl-4-methyleneisoxazolidin-5-one (MZ-6) – a new compound with α-methylene-γ-lactone motif- on two breast cancer cell lines. *Chem. biol drug des.* 79. 112-120.

Yang, H. and Ping, Dou Q. (2010). Targeting Apoptosis Pathway with Natural Terpenoids Implications for Treatment of Breast and Prostate Cancer. *Curr Drug Targets*.11 (6), 733-744.

Yao, D., Dai, C. and Peng C. (2011).Mechanism of the mesenchymal-epithelial transition and its relationship with metastatic tumor formation.*Mol Cancer Res*. 12, 1608-20.

Zhang, D., Qiu, L., Jin, X., Guo, Z. and Guo, C. (2009). Nuclear factor-κB inhibition by parthenolide potentiates the efficacy of taxol in non-small cell lung cancer *in vitro* and *in vivo.Mol cancer res*. 7, 1139-1149.

Zhang, S., Ong, C., Shen, H., (2004).Critical roles of intracellular thiols and calcium in parthenolide-induced apoptosis in human colorectal cancer cells.*Cancer Lett*. 208, 143-153.

Zhang, S., Won, Y., Ong, C. and Shen, H. (2005). Anti-cancer potential of sesquiterpene lactones: bioactivity and molecular mechanisms. *Current Medicinal Chemistry-Anti-Cancer Agents*.5, 239-249.

Zhang, S., Won, Y., Ong, C., Shen, H. (2005). Anti-cancer potential of sesquiterpene lactones: bioactivity and molecular mechanisms. *Curr Med Chem Anticancer Agents*. 5, 239–249.

Zhang, Y., Lukacova, V., Reindl, K., and Balaz, S. (2006). Quantitative characterization of binding of small molecules to extracellular matrix. *Journal of biochemical and biophysical methods*.67, 107-122.

Zhou, X-D. and Agazie, Y. (2008). Inhibition of SHP2 leadsto mesenchymal to epithelial transition in breast cancer cells.*Cell Death and Differentiation*. 15, 988-9966.

Zuo, L., Li, W. and You., S. (2010). Progesterone reverses the mesenchymal phenotypes of basal phenotype breast cancer cells via a membrane progesterone receptor mediated pathway. Breast *Cancer Res*. 12, R34.